Supporting Information

Organocatalyzed Bottom-up Formation of Protocells

Marian Simon Rafael Ebeling,[1] Otto Berninghausen,[2] Khang Hoang Nguyen,[1] Roland Beckmann,[2] Oliver Trapp[1,3,*]

[1]Department of Chemistry, Ludwig-Maximilians-University Munich, Munich, Germany.
[2]Department of Biochemistry, Gene Center, Ludwig-Maximilians-University Munich, Munich, Germany
[3]Max Planck Institute for Astronomy, Heidelberg, Germany

*Corresponding author: Email: oliver.trapp@cup.uni-muenchen.de

Contents

Supplementary Figures

Supplementary Tables

List of abbreviations

AGC-target	Automatic gain control target
cryo-TEM	Cryogenic transmission electron microscopy
DCM	Dichloromethane
D_h	Hydrodynamic diameter
DLS	Dynamic light scattering
DMSO	Dimethyl sulfoxide
DNA	Deoxyribonucleic acid
dr	Diastereomeric ratio
ee	Enantiomeric excess
ESI	Electrospray ionization
FAS	Fatty acid synthase
FTT	Fischer-Tropsch type
HPLC	High performance liquid chromatography
HRMS	High resolution mass spectrometry
NMR	Nuclear magnetic resonance
pKa	Negative decadic logarithm of the acid dissociation constant
RNA	Ribonucleic acid
SPS	Solvent purification system
THF	Tetrahydrofuran
TEM	Transmission electron microscopy
TFA	Trifluoroacetic acid
TLC	Thin layer chromatography
UV	Ultraviolet radiation

General experimental details

1 General considerations

1.1 Techniques

Air and moisture sensitive reactions were carried out in an argon atmosphere (Ar 5.0) under exclusion of air and moisture. All glassware was flame-dried prior to use and standard Schlenk techniques were employed. Syringes to transfer liquids and solutions were flushed thrice with argon prior to use; solids were added under argon flow. If not stated otherwise, the yields given refer to isolated and purified products.

1.2 Solvents, reagents and starting materials

Anhydrous THF, DCM and Et_2O were taken from a SPS (MB SPS 5 from MBRAUN) under argon atmosphere. All other solvents and chemicals were purchased from commercial sources and stored according to the respective instructions. Isolated compounds were stored under argon and, if needed, at 5 °C or –20 °C.

1.3 Flash column chromatography

Preparative purification by flash column chromatography was performed using silica gel (technical grade, pore size: 60 Å, particle size: 35-70 µm). Thin-layer chromatography was performed using pre-coated polyester sheets (0.2 mm silica gel with fluorescent indicator). For visualization, the TLC plates were analyzed under UV-light or stained by submerging in an aqueous solution of potassium permanganate and developed by heating.

1.4 Nuclear magnetic resonance spectroscopy

^{1}H- and ^{13}C-NMR spectra were measured on a BRUKER Avance III *HD* 400 MHz spectrometer with a CryoProbe™ operating at 400 MHz for proton nuclei and 100 MHz for carbon nuclei, respectively. For NMR data processing the MESTRELAB RESARCH software MestReNova v15.0.0-34764 was used. Chemical shifts were calibrated using the residual NMR solvent signals: $CDCl_3$: ^{1}H NMR δ[ppm] = 7.26, ^{13}C NMR δ[ppm] = 77.16; DMSO-d_6: ^{1}H NMR δ[ppm] = 2.50, ^{13}C NMR δ[ppm] = 39.52, CD_3OD: ^{1}H NMR δ[ppm] = 3.31, ^{13}C NMR δ[ppm] = 49.0.[1] All ^{13}C spectra were recorded with ^{1}H decoupling. The following abbreviations were used for multiplicity: s (singlet), d (doublet), t (triplet), q (quartet), p (pentet), m (multiplet) and bs (broad singlet). Coupling constants through n bonds (^nJ) are provided in Hertz [Hz]. The assignment of the signals was realized by two-dimensional NMR spectroscopy (^{1}H-^{1}H-COSY, ^{1}H-^{13}C-HSQC, ^{1}H-^{13}C HMBC).

1.5 High resolution mass spectroscopy

High resolution mass spectrometric (HRMS) analysis was performed using a THERMO SCIENTIFIC Q Exactive Plus mass spectrometer coupled to electrospray ionization (ESI). The mass spectrometer was operated with a scan range of 100 to 750 *m/z* in positive mode with a resolution of 140,000 and an AGC-target of $1 \cdot 10^6$. The auxiliary gas heater was set to 150 °C, the capillary temperature was set to 250 °C and spray voltage was set to 3.5 kV. For measurements, samples were eluted in the flow of H_2O/*i*-PrOH/TFA (80:20:0.5 %).

1.6 Dynamic light scattering

A VISCOTEK 802 DLS setup was used with the cell temperature set to 20 °C. The laser intensity was automatically adjusted to 300,000 counts continuously before every measurement. The data was analyzed using the software OmniSIZE version 3.0.0.296 from VISCOTEK.

1.7 High performance liquid chromatography - Analysis

HPLC measurements were performed on an AGILENT Series 1200 Infinity system equipped with a high-performance autosampler model HiP-ALS SL+ and a G1315D photodiode array detector (DAD) coupled to a 6120 Quadrupole LC/MS detector with atmospheric-pressure chemical ionization (APCI). The separation of different imidazolidine-4-thione derivatives and precursors was performed with a CHIRALPAK® IC (ID 4.6 mm x 250 mm, particle size 5 µm) or CHIRALPAK® IC-3 (ID 4.6 mm x 150 mm, particle size 3 µm) from DAICEL at 20 °C and a flow of 1.00 mL/min. 5 µL of the sample was injected and eluted using a mixture of *n*-hexane/*i*-PrOH (80/20). The peaks were detected at 270 nm. HPLC grade solvents were purchased from Sigma-Aldrich.

1.8 Ultrapure water

Ultrapure water used for experiments and measurements was obtained from a Puranity PU 15 UV from VWR.

1.9 Eppendorf Pipettes

For small volumes, EPPENDORF Research® plus Pipettes 0.5–10 µL, 10–100 µL, 20–200 µL and 100–1000 µL were used.

1.10 Buffer preparation

A 0.2 M carbonate/bicarbonate buffer solution for pH 9.2 was prepared by dissolving Na_2CO_3 (211.1 mg) and $NaHCO_3$ (1.51 g) in ultrapure water and filling to 100 mL volume.

1.11 pH-Titration

For pH titration a SCHOTT Instruments Lab 850 Laboratory pH Meter was used in combination with a METTLER-TOLEDO InLab®Micro with a pH range of 0–14, temperature range of 0–80 °C and the electrolyte 3 M KCl.

1.12 Light microscopy / fluorescence microscopy - experiment settings

For light microscopy and fluorescence microscopy, a ZEISS Axioscope 5 was used in combination with a monochromatic camera Axiocam 705 mono, mounted with a 0.65× adapter. Unless stated otherwise, a 100× objective EC Plan-Neofluar 100×/1.30 Oil was used. Immersol™ 518 F was used for oil immersion microscopy to increase resolving power.

80 µL of the reaction mixture was added to the cavity of a microscope slide (76 × 26 × 1.35 mm with 2 cavities Ø = 15–18 mm, depth 0.6–0.8 mm, from MARIENFIELD) and covered with a cover glass (thickness no. 1½, high-performance, 18 mm x 18 mm, 0.170 ± 0.005 mm, from ZEISS).

For fluorescence microscopy, a HXP 120 V fluorescence light source was used in combination with the filter set 43 HE from ZEISS. Excitation: BP 550/25 (HE), Beamsplitter: FT 570 (HE) and Emission: BP 605/70 (HE). For sample preparation, 90 µL of the reaction mixture was mixed with 10 µL of the fluorescent dye rhodamine B (1 µM), then 80 µL were taken and added to the cavity of a microscope slide and covered with a cover glass. For extended observation times during (fluorescence)-experiments, the glass cover was sealed with clear nail polish or high vacuum grease to prevent evaporation of volatiles.

1.13 (cryo)-TEM – sample preparation and measurement

3.5 µl of the reaction mixture was applied to 2 nm pre-coated Quantifoil R3/3 holey carbon-supported grids or to molybdenum grids coated with lacey carbon films (200 mesh) and either vitrified using Vitrobot Mark IV (FEI/THERMOFISHER) or negatively stained using 2 % uranyl acetate. Negative stained grids were analysed using a Megaview 1024 × 1024 pixel CCD camera (iTEM) at different magnifications on a Morgagni TEM (THERMO FISHER SCIENTIFIC) at 80 kV. Images of vitrified samples were collected under low dose conditions at various nominal magnifications using EM-TOOLS (TVIPS GmbH) on a Tecnai G2 Spirit transmission electron microscope (THERMO FISHER SCIENTIFIC) equipped with a F218 2048 × 2048 pixel CCD camera (TVIPS GmbH) at 120 kV.

2 Synthetic, spectroscopic, and analytical data

2.1 Retrosynthetic pathway to the reference (5*S*)-2,5-dimethylimidazolidine-4-thione (1)

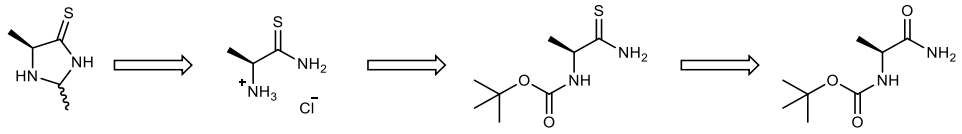

Scheme S1 General retrosynthetic pathway to imidazolidine-4-thiones from boc-protected alanine.

2.1.1 Synthesis of *tert*-butyl (*S*)-(1-amino-1-thioxopropan-2-yl)carbamate (9)

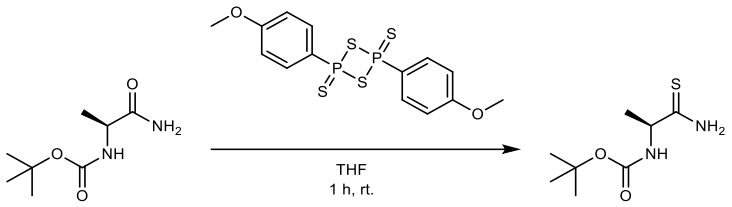

Scheme S2 Synthesis of tert-butyl (*S*)-(1-amino-1-thioxopropan-2-yl)carbamate (9) using Lawesson's reagent.

tert-Butyl (*S*)-(1-amino-1-oxopropan-2-yl)carbamate (3.76 g, 20.0 mmol, 1.00 equiv.) and LAWESSON'S reagent (4.45 g, 11.0 mmol, 0.55 equiv.) were dissolved in dry THF (100 mL) and were stirred under argon for 1 h. All volatiles were removed *in vacuo*. The crude product was purified by flash column chromatography (*n*-pentane/EtOAc, 5:2 to 1:1) to obtain **9** (2.80 g, 68 %) as a white solid.

^{1}H NMR (400 MHz, DMSO-d_6) δ [ppm] = 9.57 (bs, 1H), 9.09 (bs, 1H), 6.83 (d, *J* = 7.6 Hz, 1H), 4.24 (m, 1H), 1.37 (s, 9H), 1.23 (d, *J* = 7.0 Hz, 3H).

^{13}C NMR (101 MHz, DMSO-d_6) δ [ppm] = 209.5, 154.6, 78.2, 55.7, 28.2, 21.1.

HRMS (HESI): found: $[M+H]^+$ 205.1007, $C_8H_{17}N_2O_2S^+$ requires 205.1005.

HPLC (IC, *n*-hexane/*i*-PrOH 80:20, 20 °C): 5.1 min.

R_f (*n*-pentane/EtOAc, 5:2) = 0.2.

2.1.2 Synthesis of (*S*)-2-aminopropanethioamide hydrochloride (8-HCl)

Scheme S3 Synthesis of (*S*)-2-aminopropanethioamide hydrochloride (8-HCl) by boc-deprotection using HCl in Et_2O.

tert-Butyl (*S*)-(1-amino-1-thioxopropan-2-yl)carbamate (2.63 g, 12.9 mmol, 1.00 equiv.) was dissolved in dry DCM (40 mL) under argon. HCl in Et_2O (2.0 M, 25.7 mL, 4.00 equiv.) was added and the solution stirred for 2 h. The solution was filtered off and the precipitate washed with dry Et_2O (3 × 20 mL) under argon. The precipitate was dried under high vacuum. The product **8-HCl** (1.66 g, 92 %) was obtained as a white solid and stored under argon.

^{1}H NMR (400 MHz, CD_3OD) δ [ppm] = 4.18 (q, *J* = 6.8 Hz, 1H), 1.52 (d, *J* = 6.5 Hz, 3H).

^{13}C NMR (101 MHz, CD_3OD) δ [ppm] = 206.8, 54.9, 21.3.

HRMS (HESI): found: $[M+H]^+$ 105.0485, $C_3H_9N_2S^+$ requires 105.0481.

2.1.3 Synthesis of (5*S*)-2,5-dimethylimidazolidine-4-thione (1)

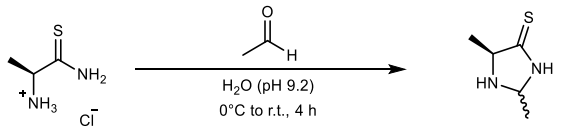

Scheme S4 Synthesis of (2*RS*,5*S*)-2,5-dimethylimidazolidine-4-thione (1) by condensation of acetaldehyde in basic conditions.

(*S*)-2-Aminopropanethioamide hydrochloride **8-HCl** (148 mg, 1.05 mmol, 1.00 equiv.) was dissolved in an aqueous $NaHCO_3/Na_2CO_3$ buffer (0.2 M, 5 mL, pH 9.2) at 0 °C. Acetaldehyde (70.0 µL, 1.26 mmol, 1.20 equiv.) was added and stirred for 90 min. Then, additional acetaldehyde (205 µL, 3.68 mmol, 3.50 equiv.) was added and the reaction was allowed to warm to room temperature. After 2 h, all volatiles were removed in vacuo. The crude product was purified by flash column chromatography (EtOAc, R_f = 0.20) to obtain **1** (87.4 mg, 762 µmol, 64 %, *dr* = 1.05) as a white solid.

Anti-diastereomer:

^{1}H NMR (400 MHz, $CDCl_3$) δ [ppm] = 9.47 (bs, 1H), 4.77 (qd, *J* = 5.8, 1.7 Hz, 1H), 3.78 (qd, *J* = 6.8, 1.7 Hz, 1H), 1.90 (br. s, 1H), 1.48 (d, *J* = 6.8 Hz, 3H), 1.44 (d, *J* = 5.8 Hz, 3H).

^{13}C NMR (101 MHz, $CDCl_3$) δ [ppm] = 207.6, 72.4, 67.2, 20.6, 19.1.

HPLC (IC-3, *n*-hexane/*i*-PrOH 95:5, 20 °C): t = 16.4 min.

Syn-diastereomer:

^{1}H NMR (400 MHz, $CDCl_3$) δ [ppm] = 9.47 (br. s, 1H), 4.91 (qd, *J* = 6.0, 1.2 Hz, 1H), 4.00 (qd, *J* = 7.0, 1.3 Hz, 1H), 1.90 (br. s, 1H), 1.41 (d, *J* = 7.1 Hz, 3H), 1.39 (d, *J* = 6.0 Hz, 3H).

^{13}C NMR (101 MHz, $CDCl_3$) δ [ppm] = 207.0, 72.8, 66.7, 21.2, 19.1.

HPLC (IC-3, *n*-hexane/*i*-PrOH 95:5, 20 °C): t = 25.7 min.

HRMS (HESI): found: $[M+H]^+$ 131.0637, $C_5H_{11}N_2S^+$ requires 131.0637.

2.2 pH Titration of (2*RS*,5*S*)-2,5-dimethylimidazolidine-4-thione (1)

Catalyst **1** (6.5 mg, 50.0 µmol, 1.00 equiv.) was dissolved in aq. NaOH (0.1 M, 1.00 mL, 50.0 µmol, 1.00 equiv). The initial pH was measured, and the solution was titrated in 2.5 µL or 5 µL steps with aq. HCl (1.0 M). The pKa values were determined using the second derivative of the titration curve. For the thiolactam we found a pKa_1 of 3.8 and for the secondary amine a pKa_2 of ~11.1. The buffering from the thiolactam at around pH 4 is also the optimal pH range for enamine formation. This emphasizes the synergy of the organocatalytic secondary amine and the thiolactone found in imidazolidine-4-thiones.

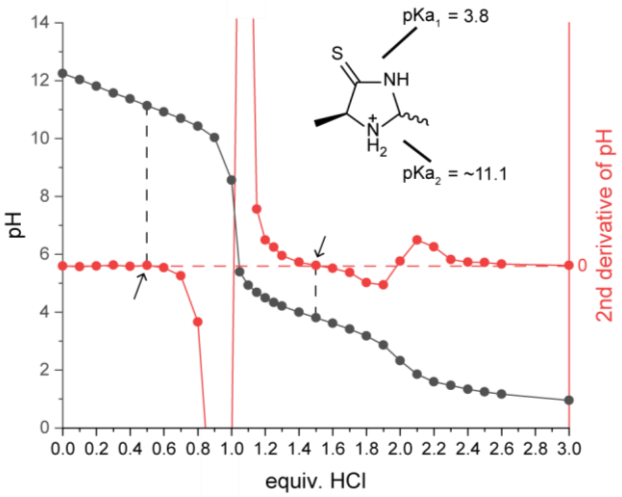

Figure S1 Titration curve of (2*RS*,5*S*)-2,5-dimethylimidazolidine-4-thione (**1**) using 1.0 M HCl. pKa_1 = 3.8, pKa_2 ≈ 11.1.

2.3 Organocatalyzed aldol oligomerization of acetaldehyde

2.3.1 General procedure - GP1

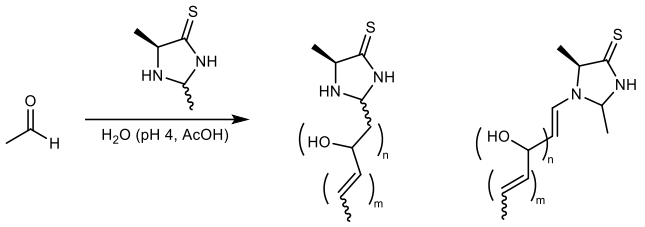

Scheme S5 Oligomerization and incorporation of acetaldehyde catalyzed by (2*RS*,5*S*)-2,5-dimethylimidazolidine-4-thione (**1**) at pH 4.

The catalyst (2*RS*,5*S*)-2,5-dimethylimidazolidine-4-thione (**1**) was added and dissolved in H_2O which was adjusted to pH 4 with acetic acid. When the solution turned clear, acetaldehyde was added, the vial tightly closed, and the solution stirred at room temperature.

Table S1 List of reaction conditions for organocatalyzed aldol oligomerization of acetaldehyde with respective amounts of reagents.

reaction condition	acetaldehyde concentration [M]	catalyst loading [%]	acetaldehyde [µL]	water [mL]	catalyst [mg]
1	0.2	0.5	60	5.33	0.7
2	0.2	1.0	30	2.66	0.7
3	0.2	2.0	30	2.66	1.4
4	0.2	5.0	30	2.66	3.5
5	0.2	10	30	2.66	7.0
6	0.2	20	30	2.66	14
7	0.5	0.5	60	2.09	0.7
8	0.5	1.0	60	2.09	1.4
9	0.5	2.0	60	2.09	3.5
10	0.5	5.0	60	2.09	7.0
11	0.5	10	60	2.09	14
12	0.5	20	30	1.05	14
13	1.0	0.5	50	0.85	0.6
14	1.0	1.0	50	0.85	1.2
15	1.0	2.0	50	0.85	2.3
16	1.0	5.0	50	0.85	5.8
17	1.0	10	50	0.85	11.7
18	2.0	0.5	60	0.478	0.7
19	2.0	1.0	60	0.478	1.4

20	2.0	2.0	60	0.478	2.8
21	2.0	5.0	60	0.478	7.0
22	2.0	10	60	0.478	14
23	2.0	20	60	0.478	28

2.3.2 Visual observation

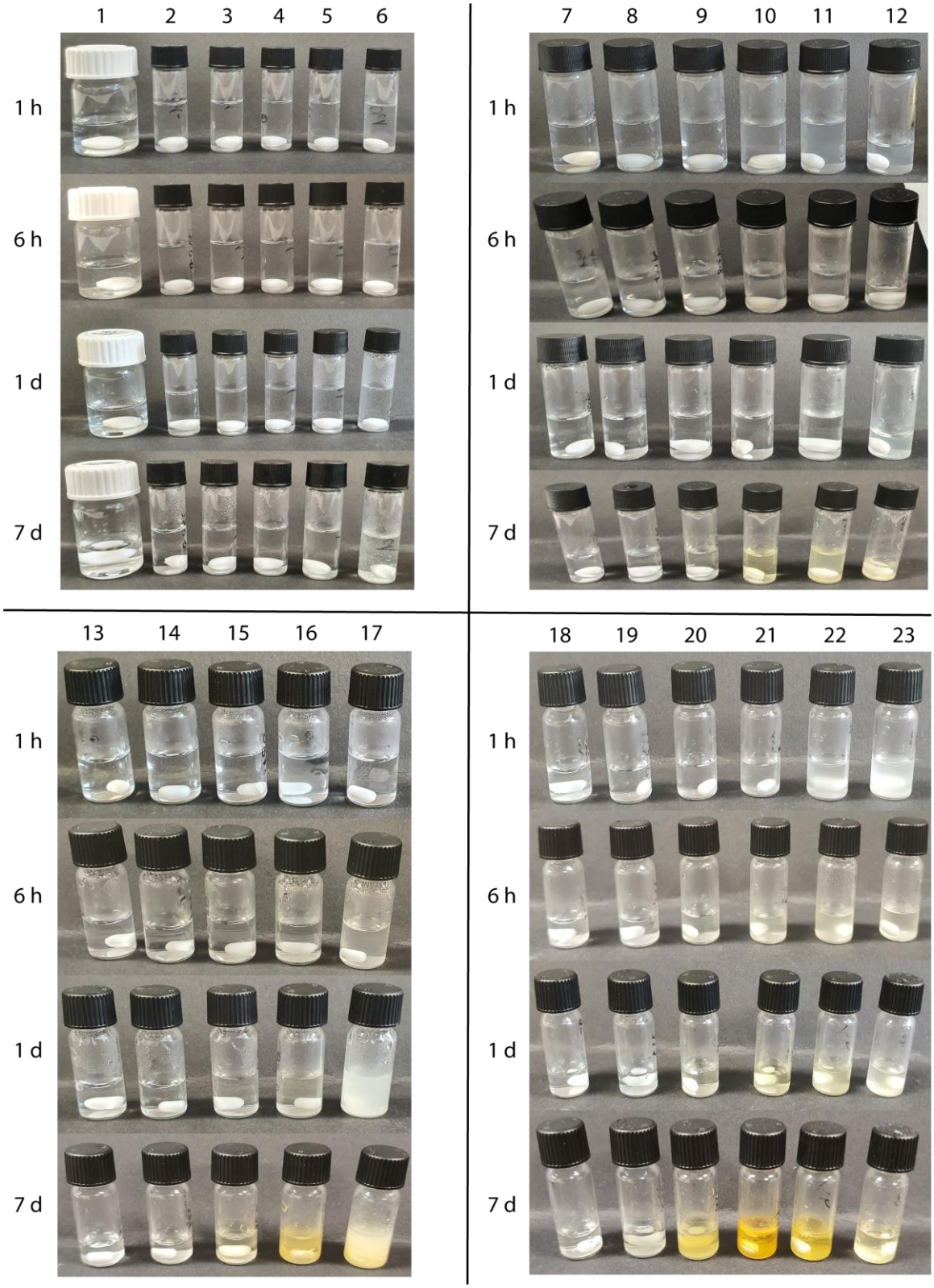

Figure S2 Pictures of reaction conditions 1–23 over time.

2.3.3 HRMS Experiments – sample preparation and analysis

For a normalized initial catalyst (**1**) concentration of 0.1 µmol/mL during the measurement, the sample volume taken was adjusted. The sample was diluted to 100 µL with ultrapure H_2O and 900 µL MeCN was added. The solution was filtered by syringe filtration using a 0.45 µm cellulose acetate *luer lock* syringe filter (red, Ø = 13 mm). The prepared solution with 0.1 µmol/mL initial catalyst (**1**) concentration was loaded into a 5 µl sample loop and injected for HRMS measurement.

Table S2 Dilution table of prebiotic reactions 1–23 to obtain 0.1 µmol/mL initial catalyst concentration for every HRMS measurement.

reaction condition	catalyst concentration	sample volume	additional water	MeCN	total sample volume
	[M]	[µL]	[µL]	[µL]	[µL]
1	0.001	100	0	900	1000
2	0.002	50.0	50.0	900	1000
3	0.004	25.0	75.0	900	1000
4	0.01	10.0	90.0	900	1000
5	0.02	5.00	95.0	900	1000
6	0.04	2.50	97.5	900	1000
7	0.0025	40.0	60.0	900	1000
8	0.005	20.0	80.0	900	1000
9	0.01	10.0	90.0	900	1000
10	0.025	4.00	96.0	900	1000
11	0.05	2.00	98.0	900	1000
12	0.1	1.00	99.0	900	1000
13	0.005	20.0	80.0	900	1000
14	0.01	10.0	90.0	900	1000
15	0.02	5.00	95.0	900	1000
16	0.05	2.00	98.0	900	1000
17	0.1	1.00	99.0	900	1000
18	0.01	10.0	90.0	900	1000
19	0.02	5.00	95.0	900	1000
20	0.04	2.50	97.5	900	1000
21	0.1	1.00	99.0	900	1000
22	0.2	1.00	199	1800	2000
23	0.4	1.00	399	3600	4000

After data acquisition, the data was averaged over 25 scans. Using a custom python program, the averaged profile data was converted to centroid data utilizing *msconvert* from ProteoWizard.[2] The peak list of the generated *.mzML-files was compared with a pre-defined $[M+H]^+$-mass-list in excel with a tolerance of 5 ppm. Found masses were reported along with their respective intensities in a new excel-file. Then, the data was visualized using the graphs below.

2.3.4 Exemplary Assignment of HRMS data

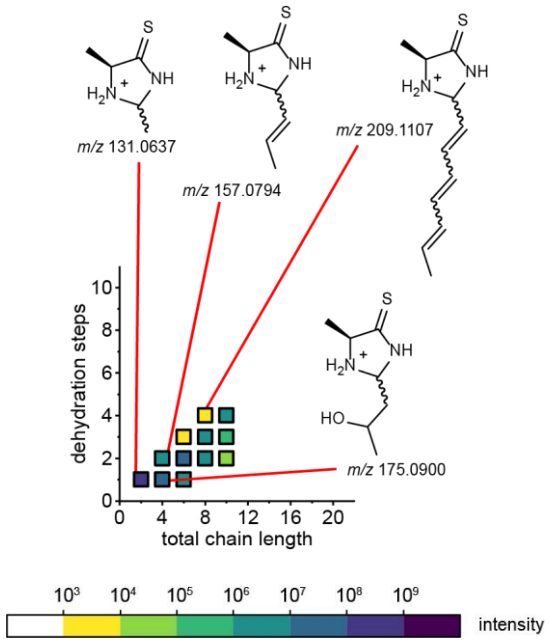

Figure S3 Exemplary assignment of HRMS data for [M+H]+ of catalysts with prolonged sidechains.

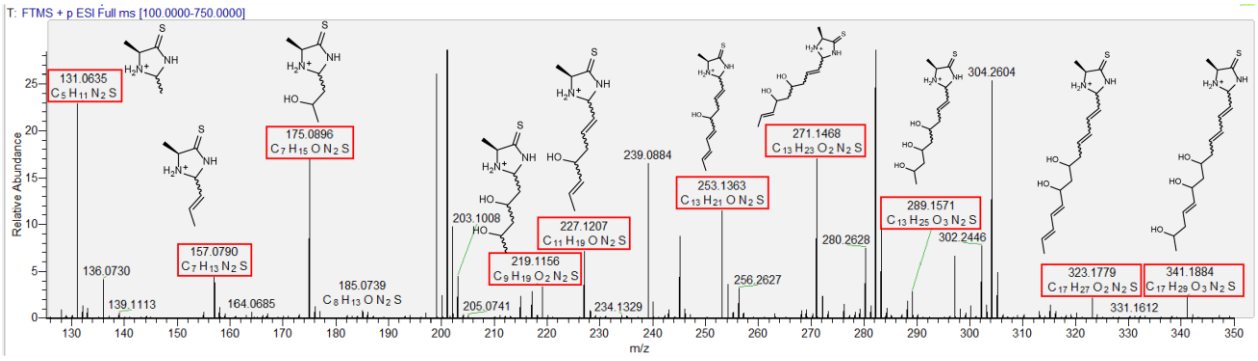

Figure S4 Exemplary HRMS spectrum with found $[M+H]^+$ masses and for each mass a possible isomer is drawn (reaction condition 20, 1 d).

2.3.5 HRMS measurements

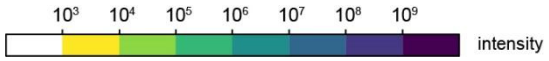

Table S3 HRMS measurements at 0.2 M acetaldehyde concentration after 1 h, 6 h, 1 d and 7 d.

no.	1 h	6 h	1 d	7 d
1	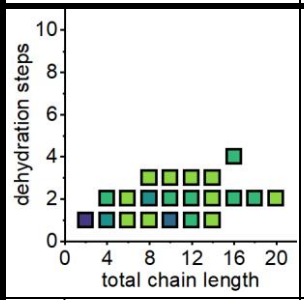	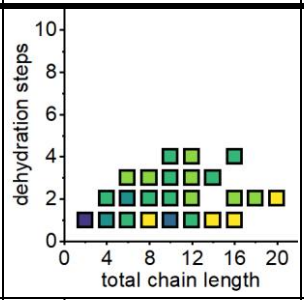	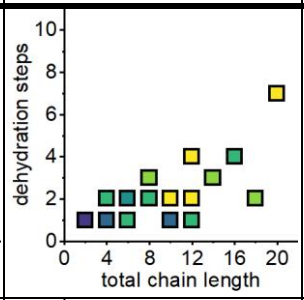	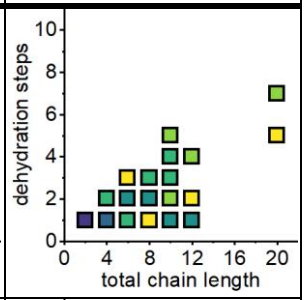
2	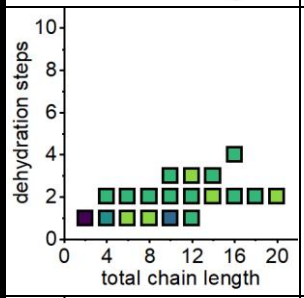	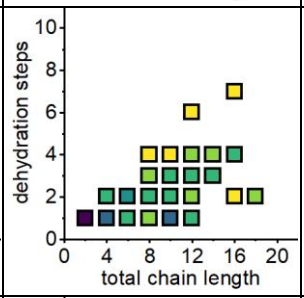	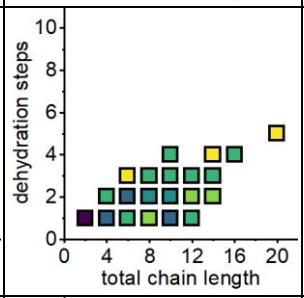	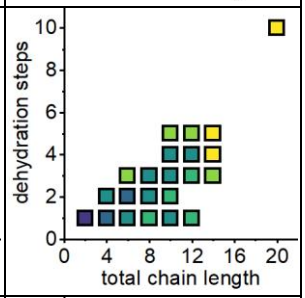
3	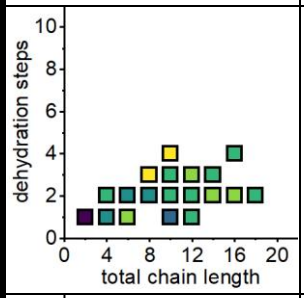	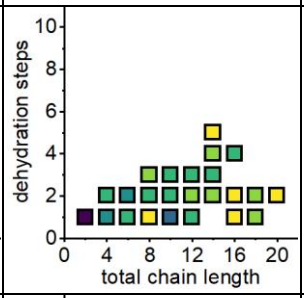	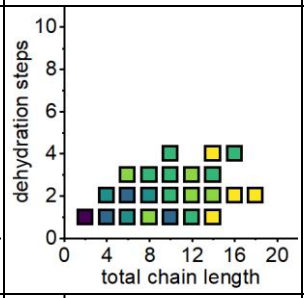	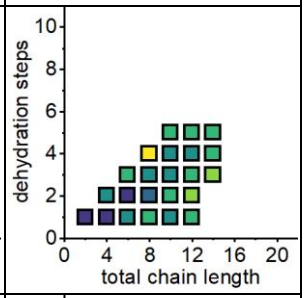
4	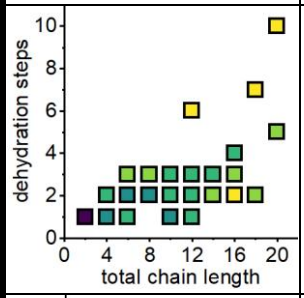	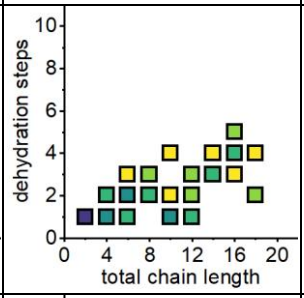	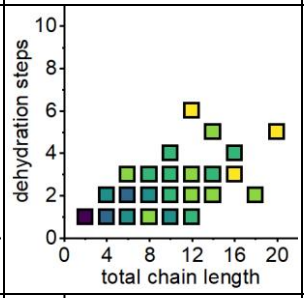	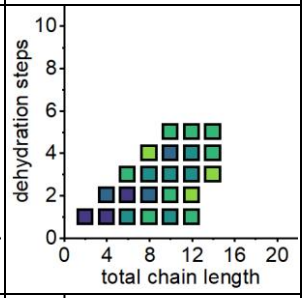
5	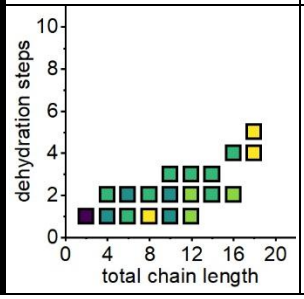	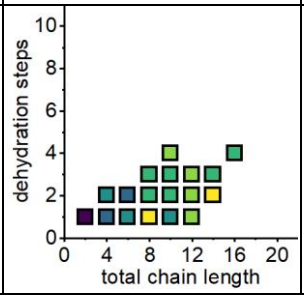	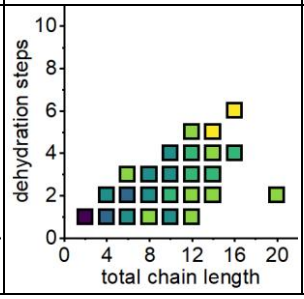	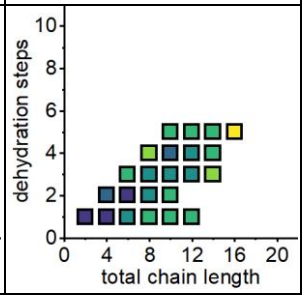

6	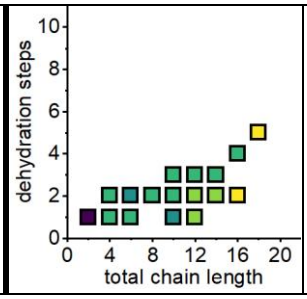 dehydration steps total chain length	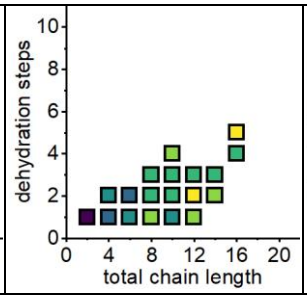 dehydration steps total chain length	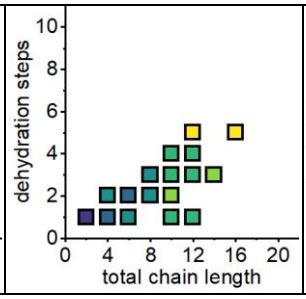 dehydration steps total chain length	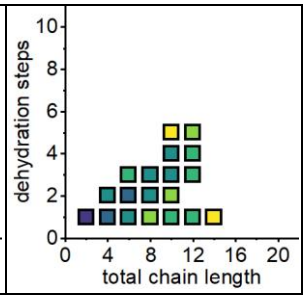 dehydration steps total chain length

Table S4 HRMS measurements at 0.5 M acetaldehyde concentration after 1 h, 6 h, 1 d and 7 d.

no.	1 h	6 h	1 d	7 d
7	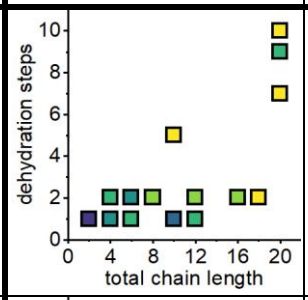	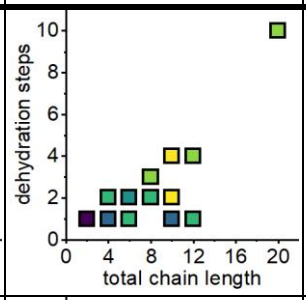	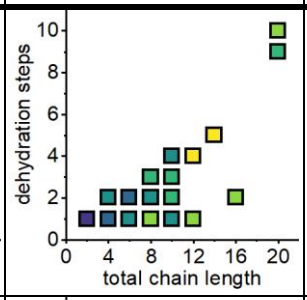	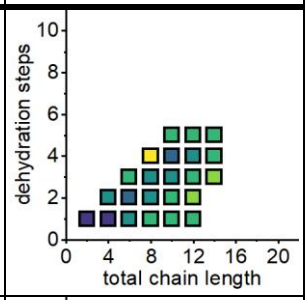
8	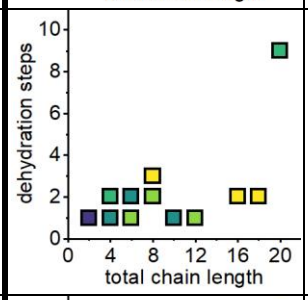	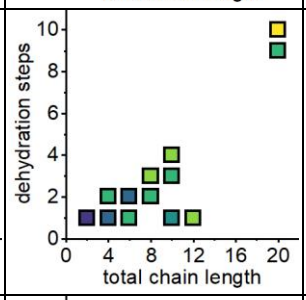	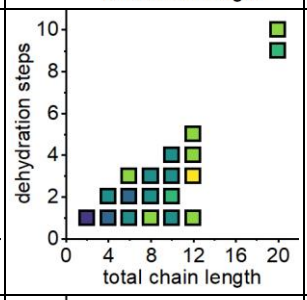	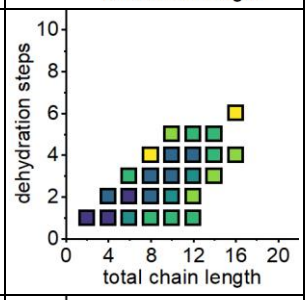
9	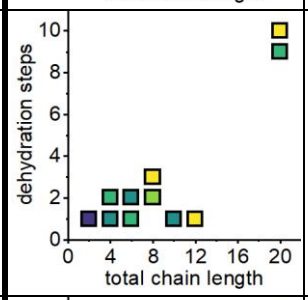	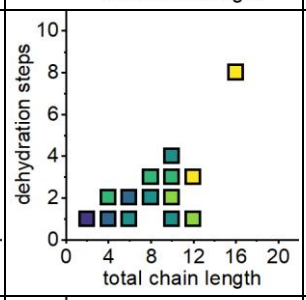	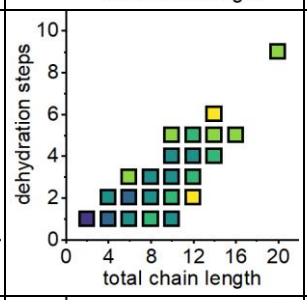	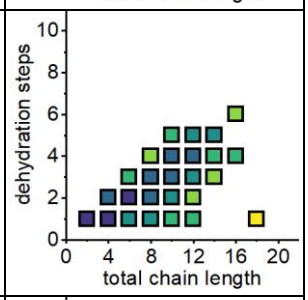
10	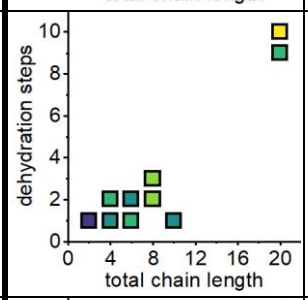	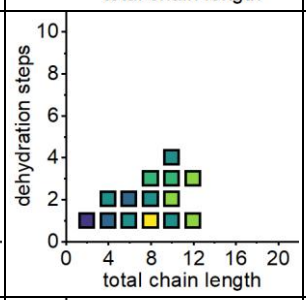	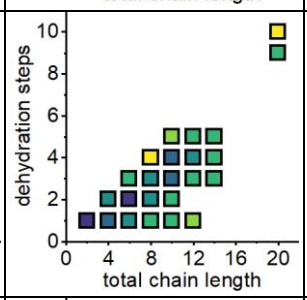	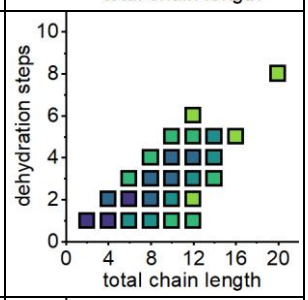
11	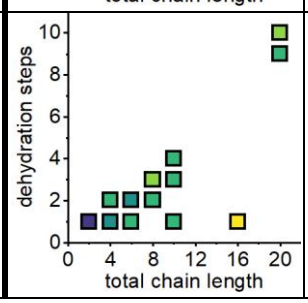	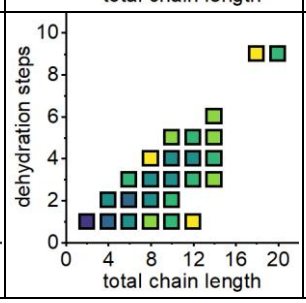	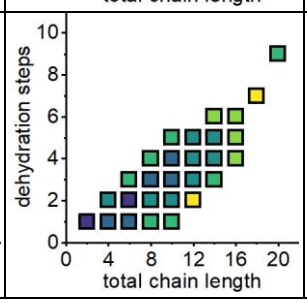	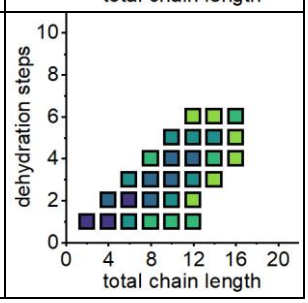

12	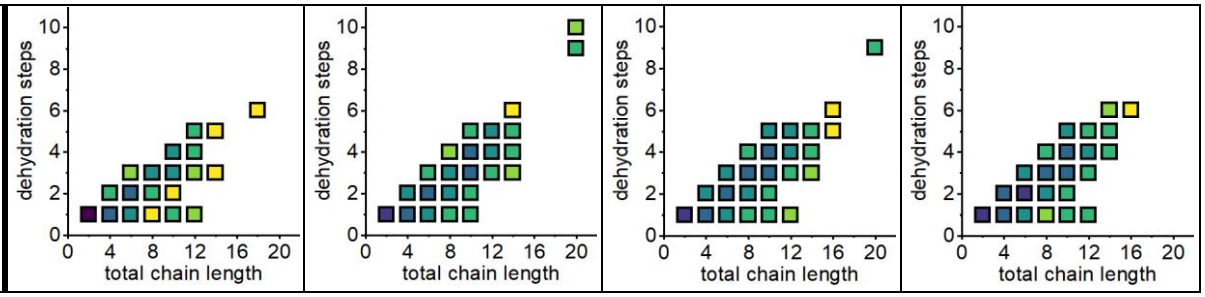			

Table S5 HRMS measurements at 1.0 M acetaldehyde concentration after 1 h, 6 h, 1 d and 7 d.

no.	1 h	6 h	1 d	7 d
13	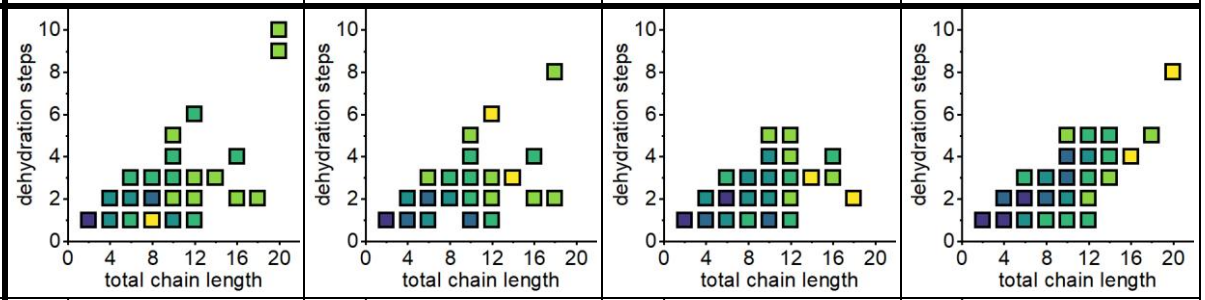			
14	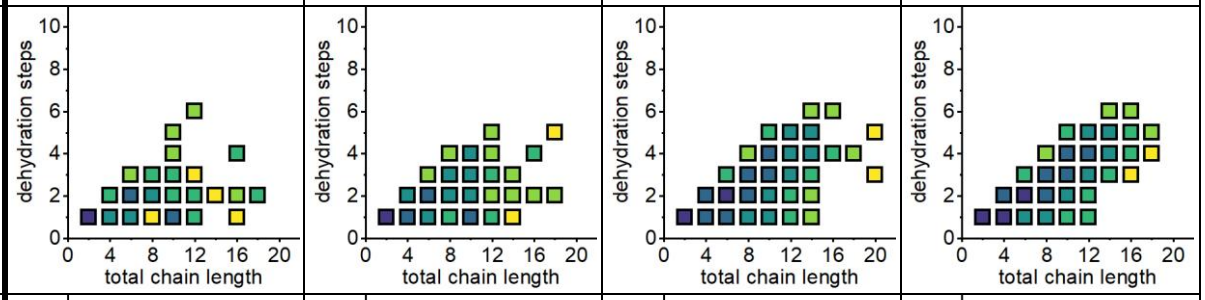			
15	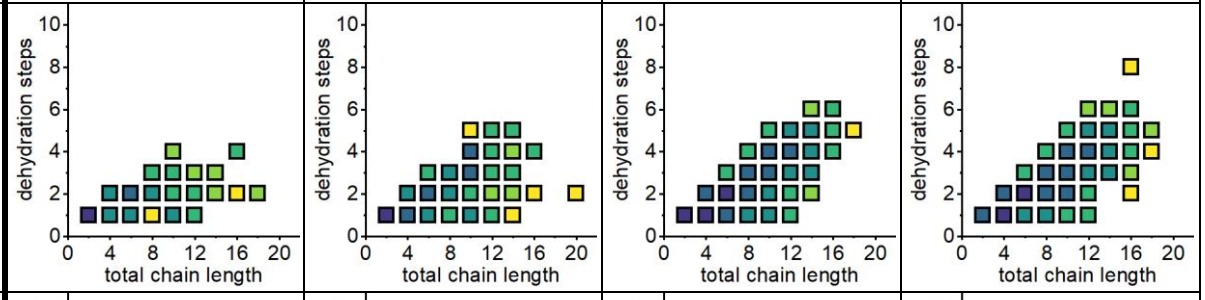			
16	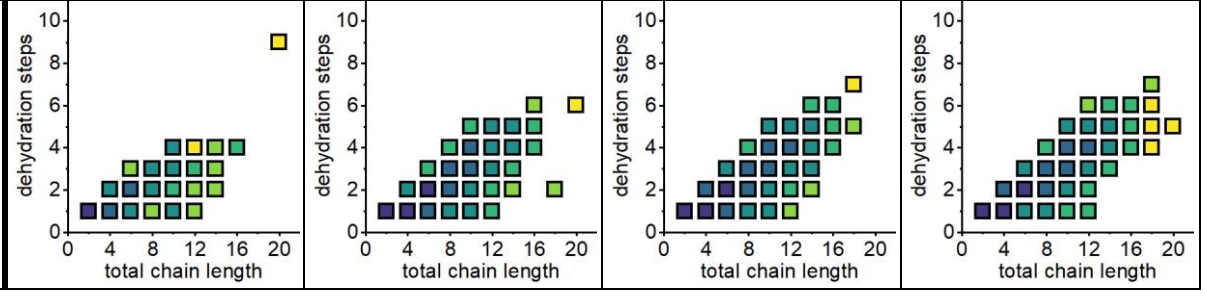			

17	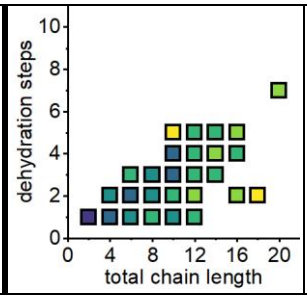 dehydration steps total chain length	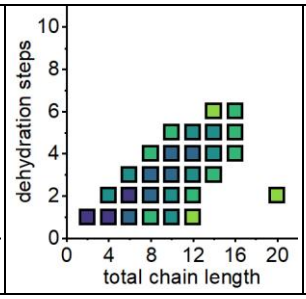 dehydration steps total chain length	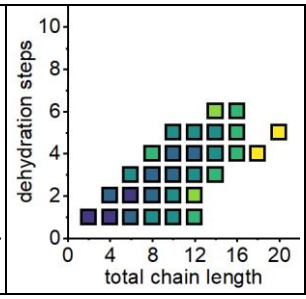 dehydration steps total chain length	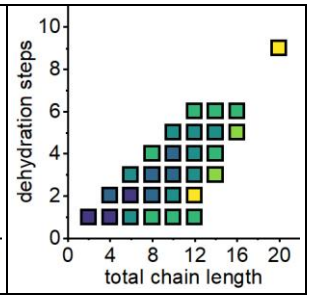 dehydration steps total chain length

Table S6 HRMS measurements at 2.0 M acetaldehyde concentration after 1 h, 6 h, 1 d and 7 d.

no.	1 h	6 h	1 d	7 d
18	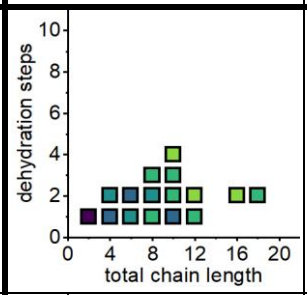	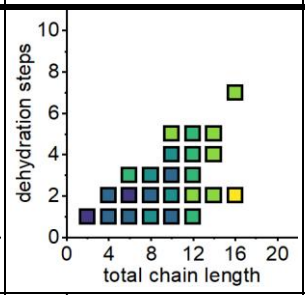	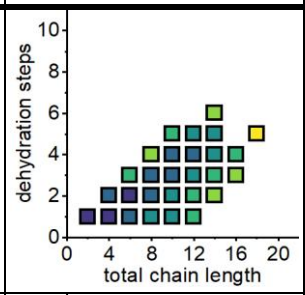	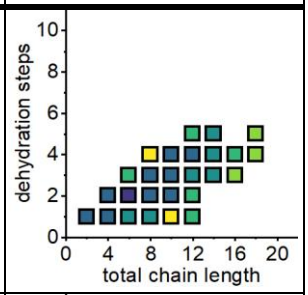
19	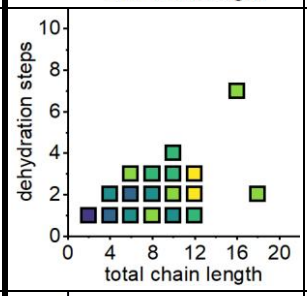	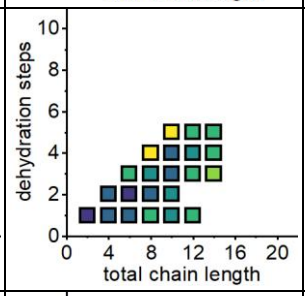	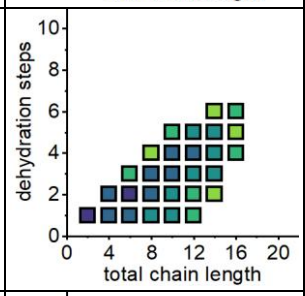	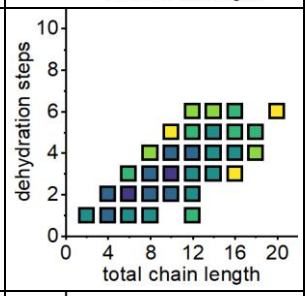
20	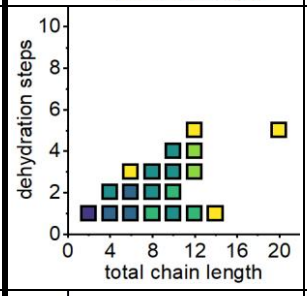	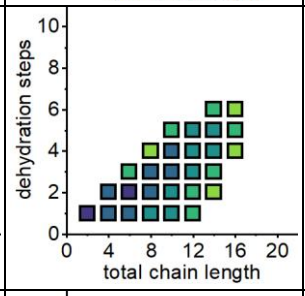	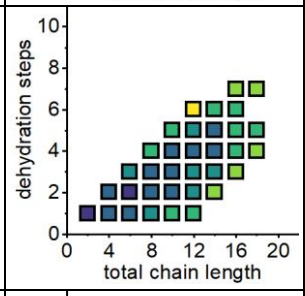	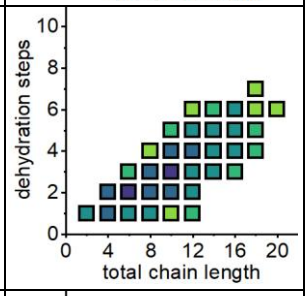
21	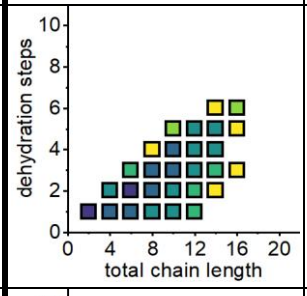	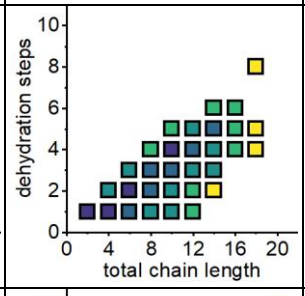	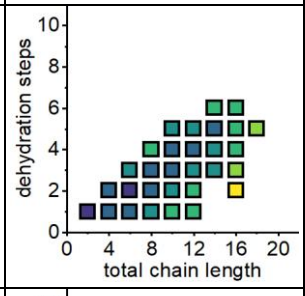	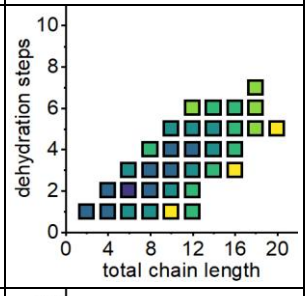
22	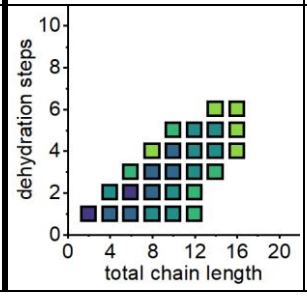	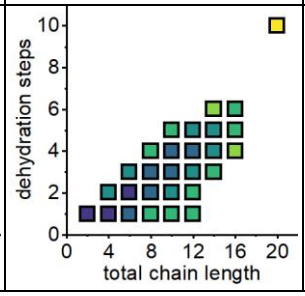	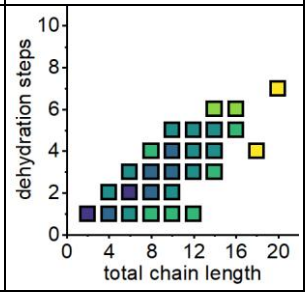	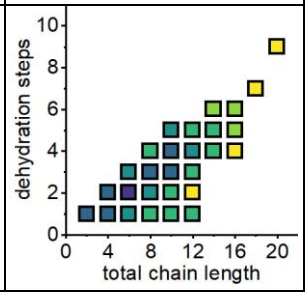

23	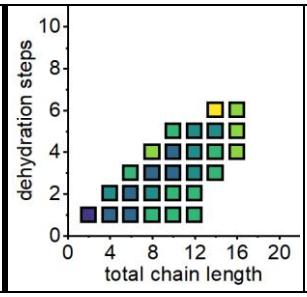 dehydration steps total chain length	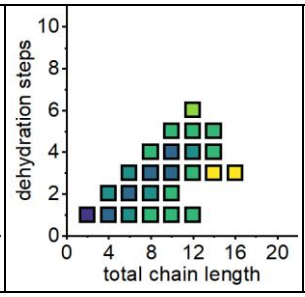 dehydration steps total chain length	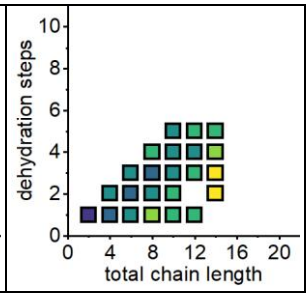 dehydration steps total chain length	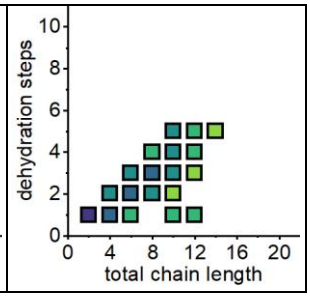 dehydration steps total chain length

2.3.6 Test of reproducibility of HRMS measurements

For every data point $[M+H]^+$ of the triplet of the same reaction condition (**Table S7**), the found intensity was averaged. When a mass was found in all three measurements, the square was outlined black (**Table S8**). For data points found in all 3 measurements, the variation coefficient was calculated and plotted accordingly in **Table S9**. Only low intensity masses were not found in every measurement and had a higher variation coefficient. The data points may vary from the measurements of reaction condition 17, as this triplet was conducted later in our study. We suspect the ambient temperature was slightly elevated which resulted in higher reactivity.

Table S7 The reaction condition 24–26 (1.0 M acetaldehyde, 10% catalyst loading, same as reaction condition 17) was started three times in succession and HRMS measurements conducted after 1 h, 6 h, 12 h and 1 d.

no.	1 h	6 h	12 h	1 d
24	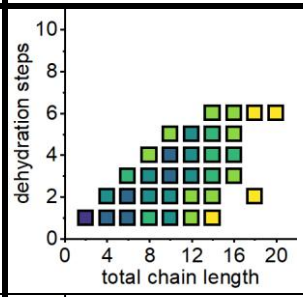	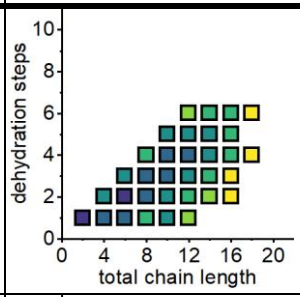	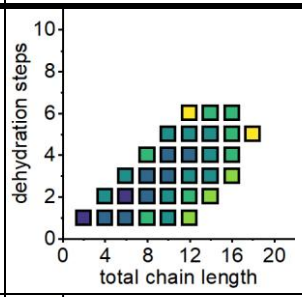	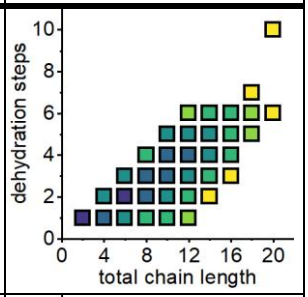
25	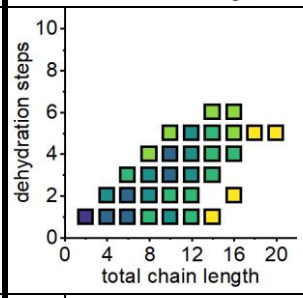	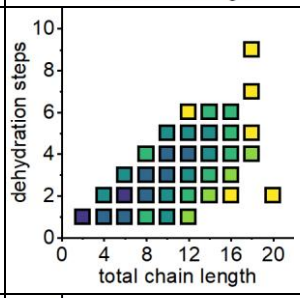	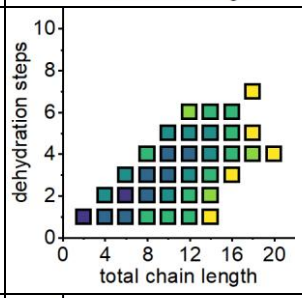	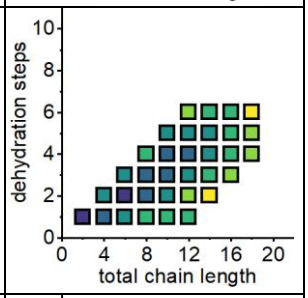
26	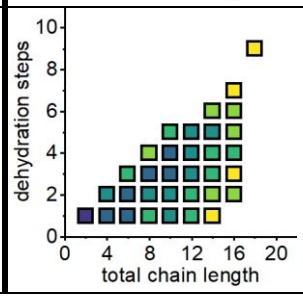	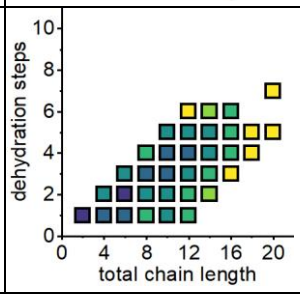	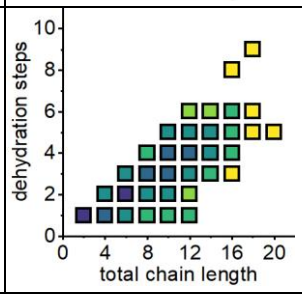	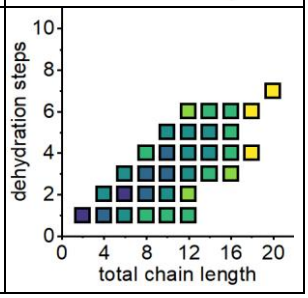

Table S8 [M+H]+ masses, which were found in every measurement in **Table S7**, were marked with a black frame.

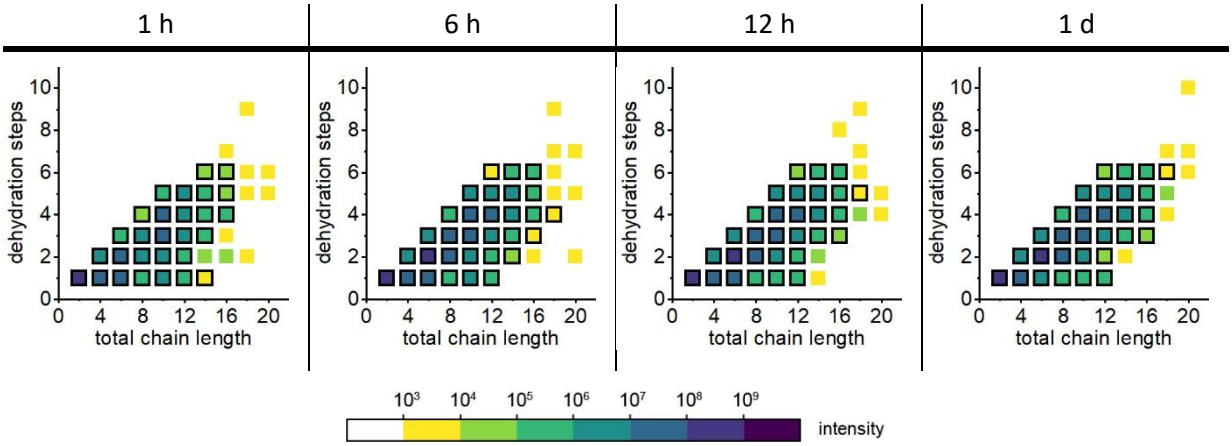

Table S9 Variation coefficient of data points of the averaged data in **Table S8**. The variation coefficient was only calculated for masses found in every measurement.

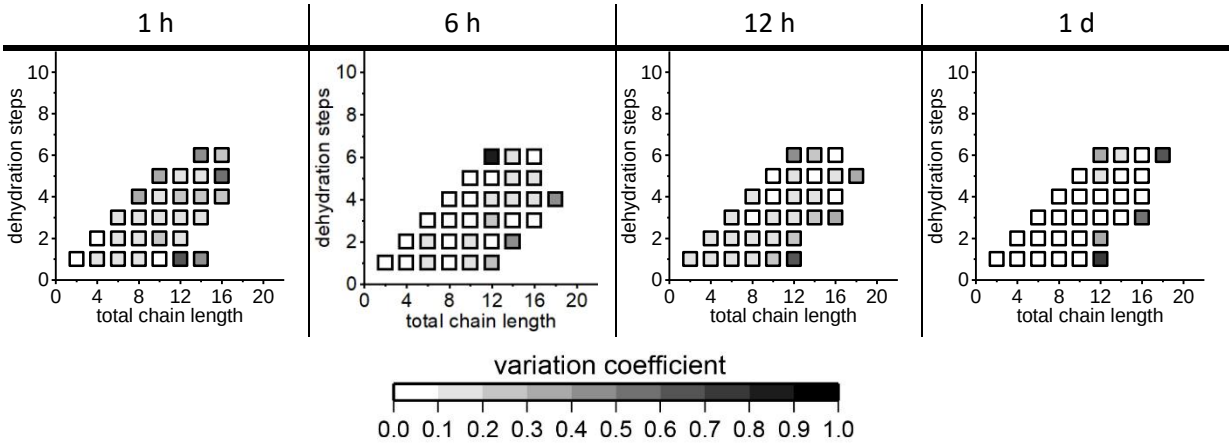

2.3.7 Microscope Micrographs

Table S10 Light micrographs at 0.2 M acetaldehyde concentration after 1 h, 6 h, 1 d and 7 d. Scale bar 20 µm.

no.	1 h	6 h	1 d	7 d
1	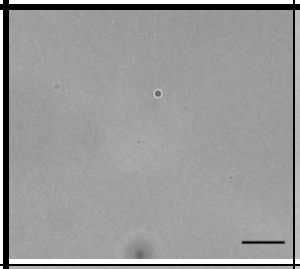	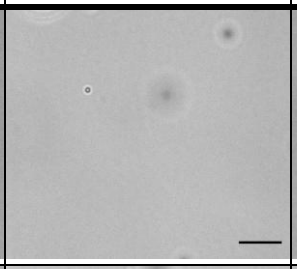	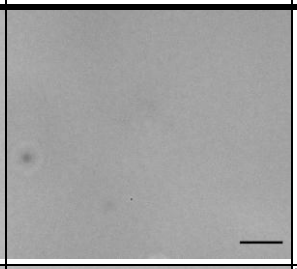	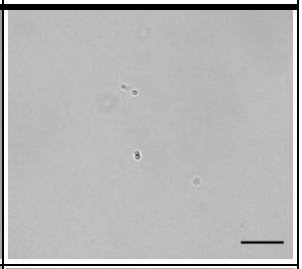
2	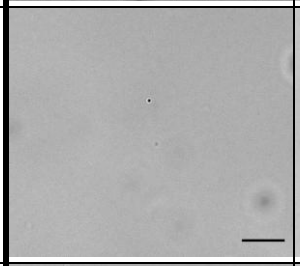	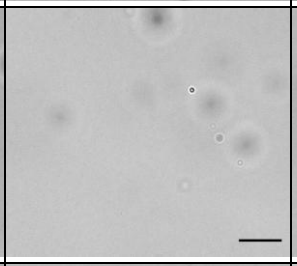	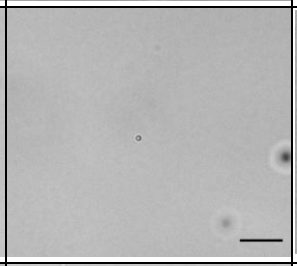	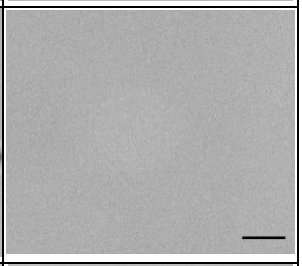
3	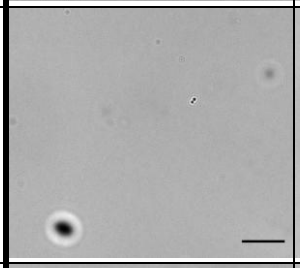	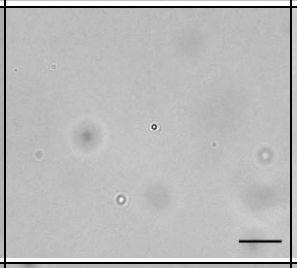	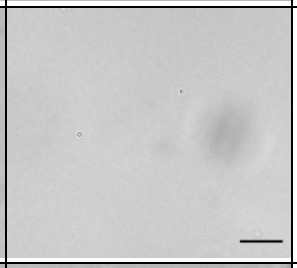	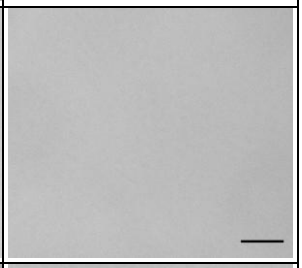
4	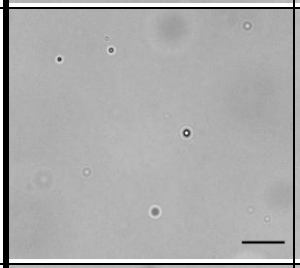	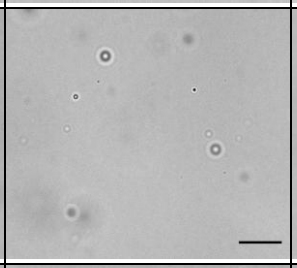	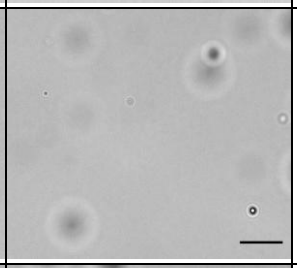	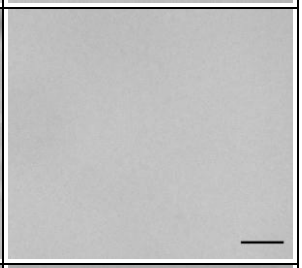
5	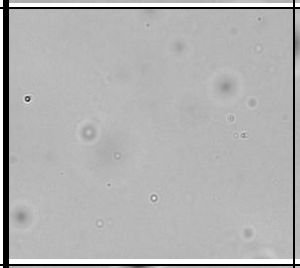	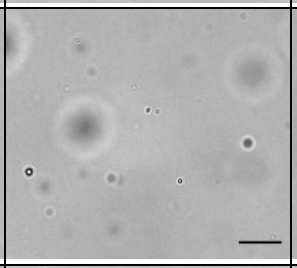	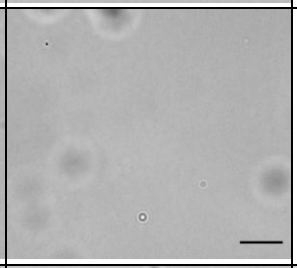	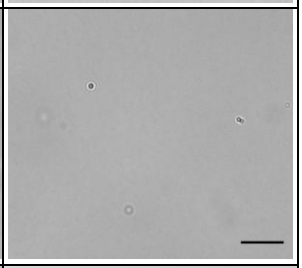
6	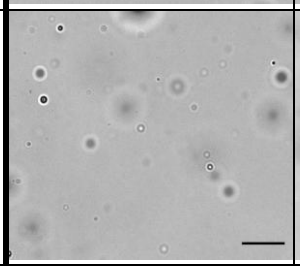	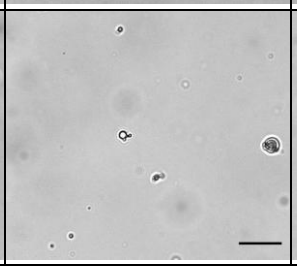	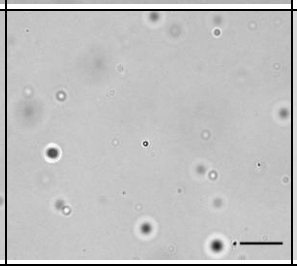	

Table S11 Light micrographs at 0.5 M acetaldehyde concentration after 1 h, 6 h, 1 d and 7 d. Scale bar 20 µm.

no.	1 h	6 h	1 d	7 d
7	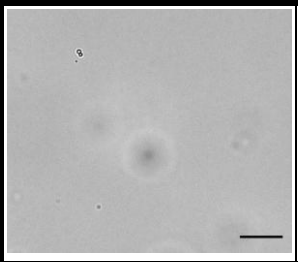	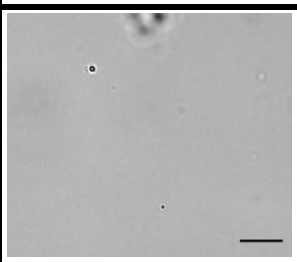	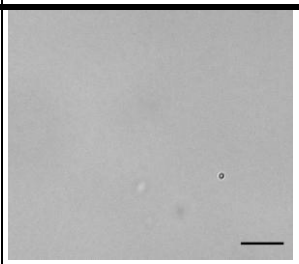	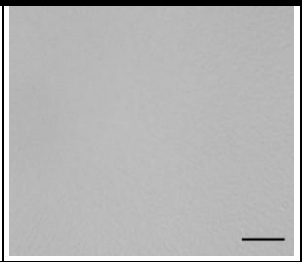
8	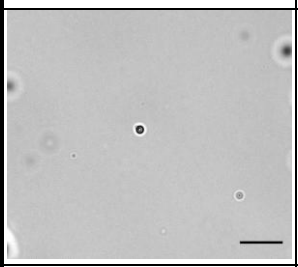	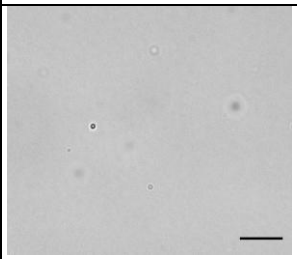	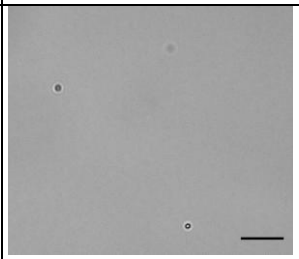	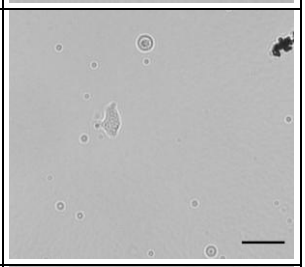
9	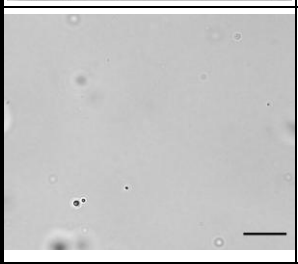	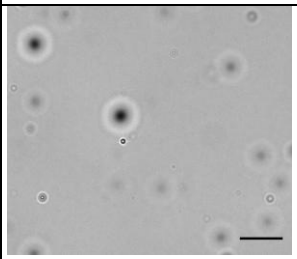	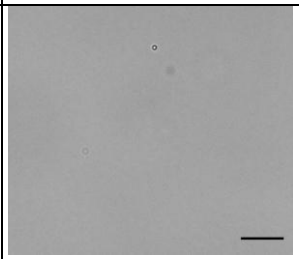	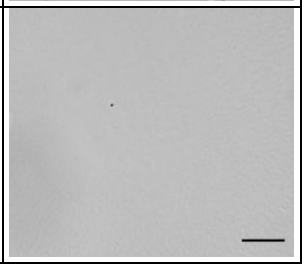
10	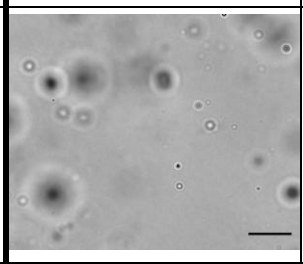	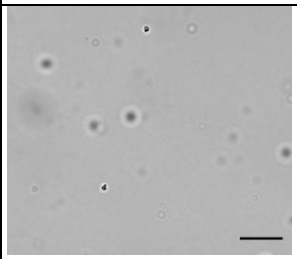	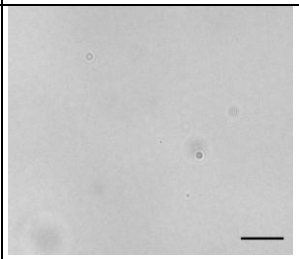	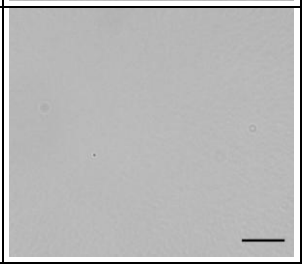
11	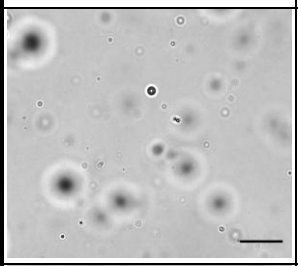	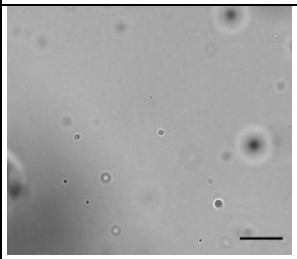	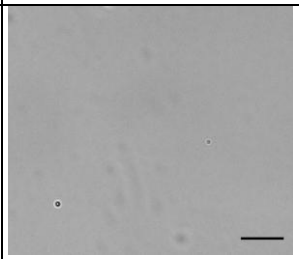	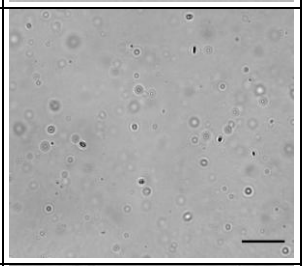
12	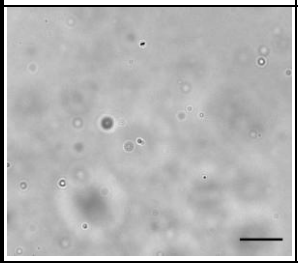	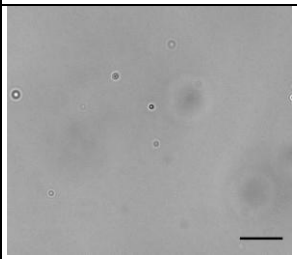	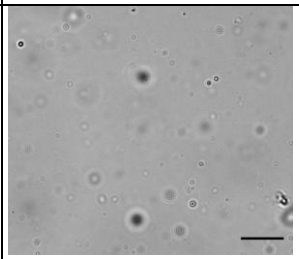	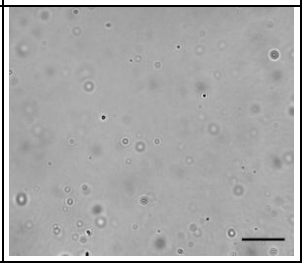

Table S12 Light micrographs at 1.0 M acetaldehyde concentration after 1 h, 6 h, 1 d and 7 d. Scale bar 20 µm.

no.	1 h	6 h	1 d	7 d
13	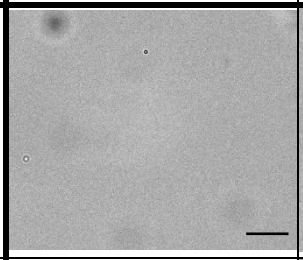	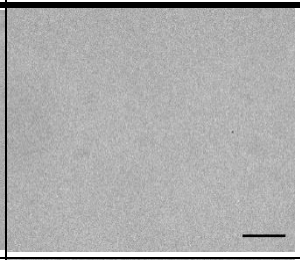	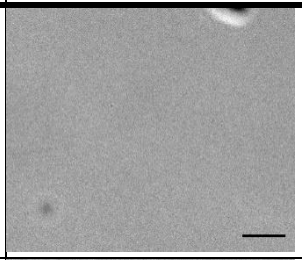	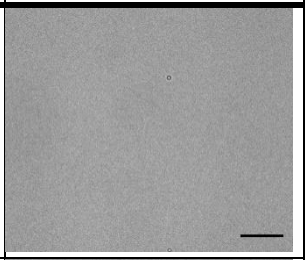
14	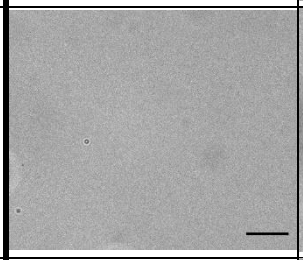	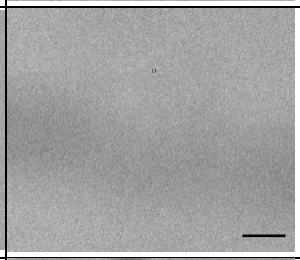	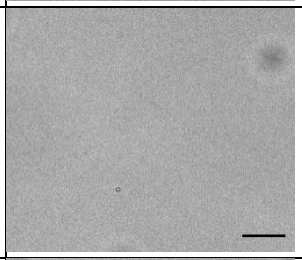	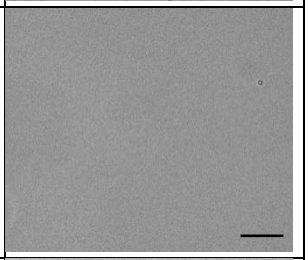
15	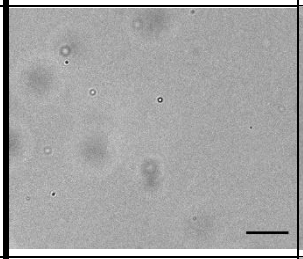	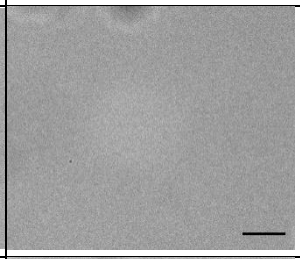	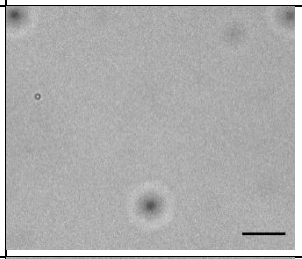	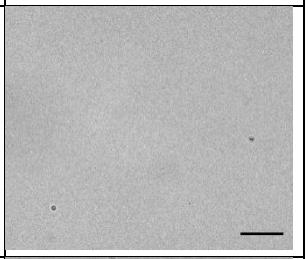
16	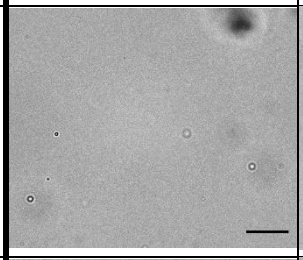	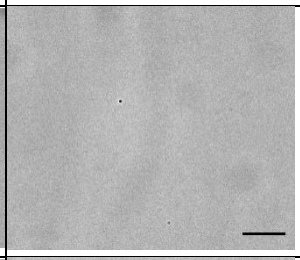	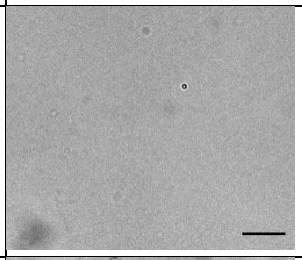	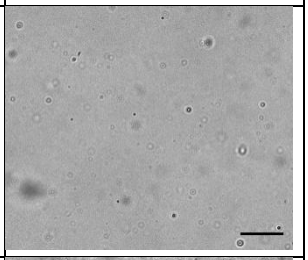
17	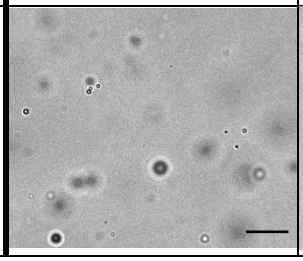	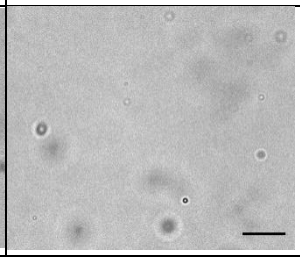	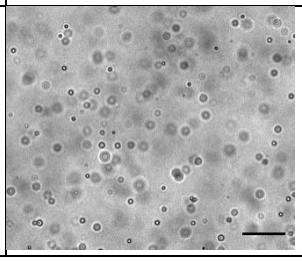	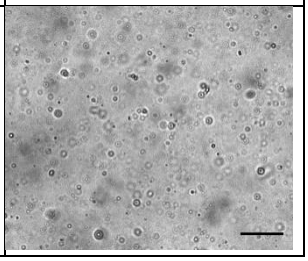

Table S13 Light micrographs at 2.0 M acetaldehyde concentration after 1 h, 6 h, 1 d and 7 d. Scale bar 20 µm.

no.	1 h	6 h	1 d	7 d
18	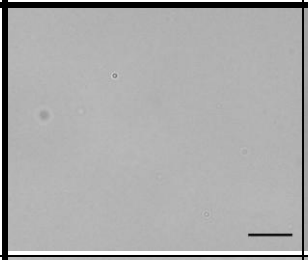	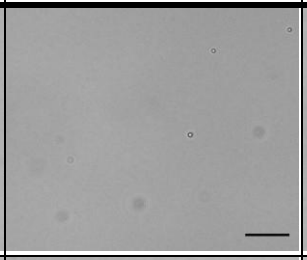	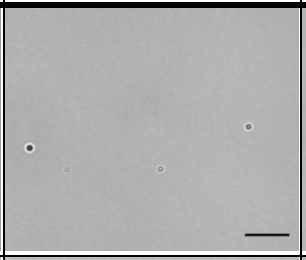	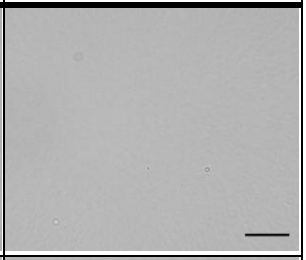
19	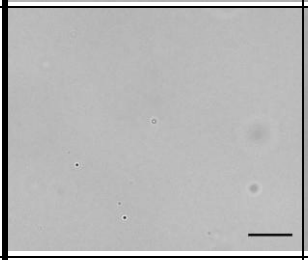	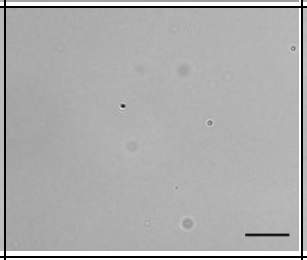	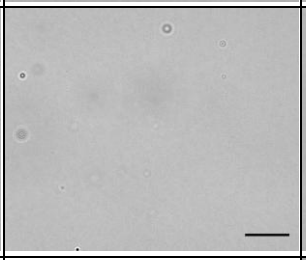	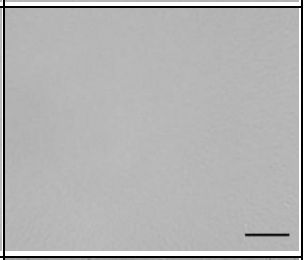
20	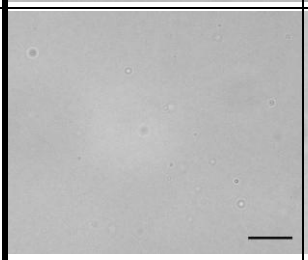	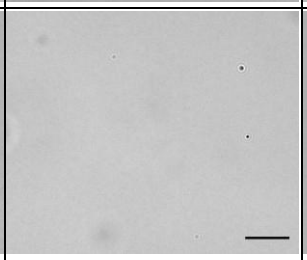	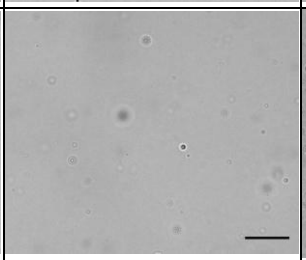	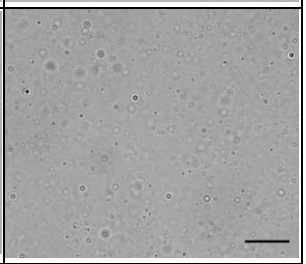
21	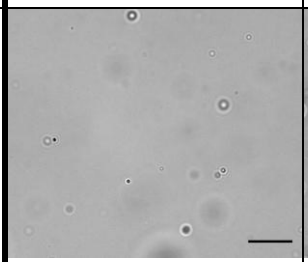	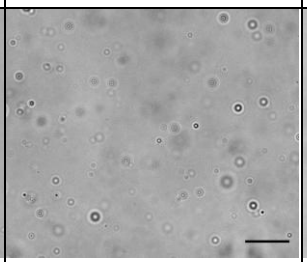	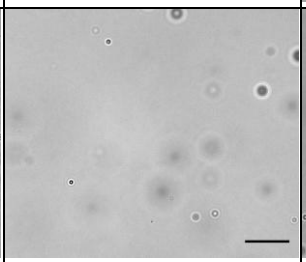	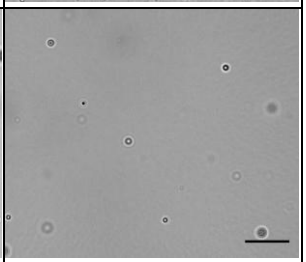
22	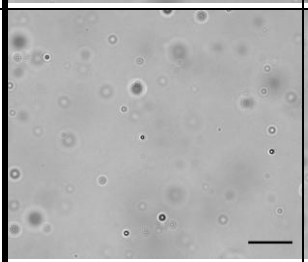	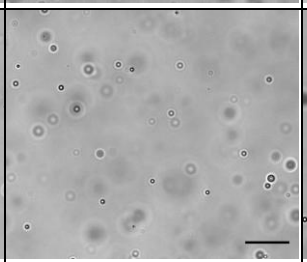	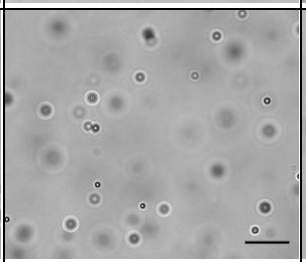	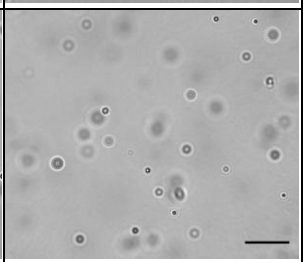
23	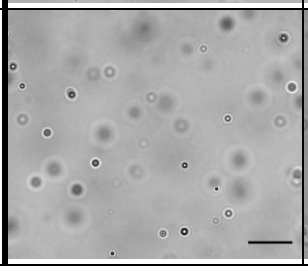	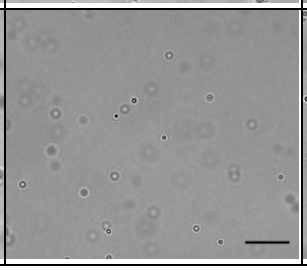	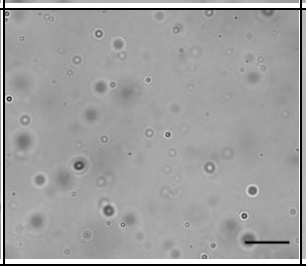	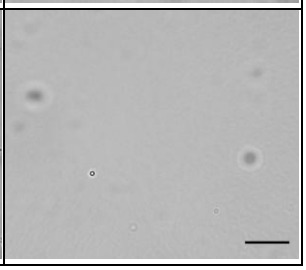

2.3.8 Fluorescence Microscopy

We used rhodamine B (0.1 μM) as a fluorescent probe to detect nonpolar regions of interest. Fluorescence is quenched in a polar environment like water. A reaction starting with 0.5 M acetaldehyde and 5% catalyst loading at room temperature was sampled after 3 h. We found different stages of coacervates next to each other in our reaction. We were able to observe the change over time, as the coacervate (uniform fluorescence) accumulates water (dark spheres) inside up to a point where a vesicle structure is formed (see Supplementary Videos 3–5).

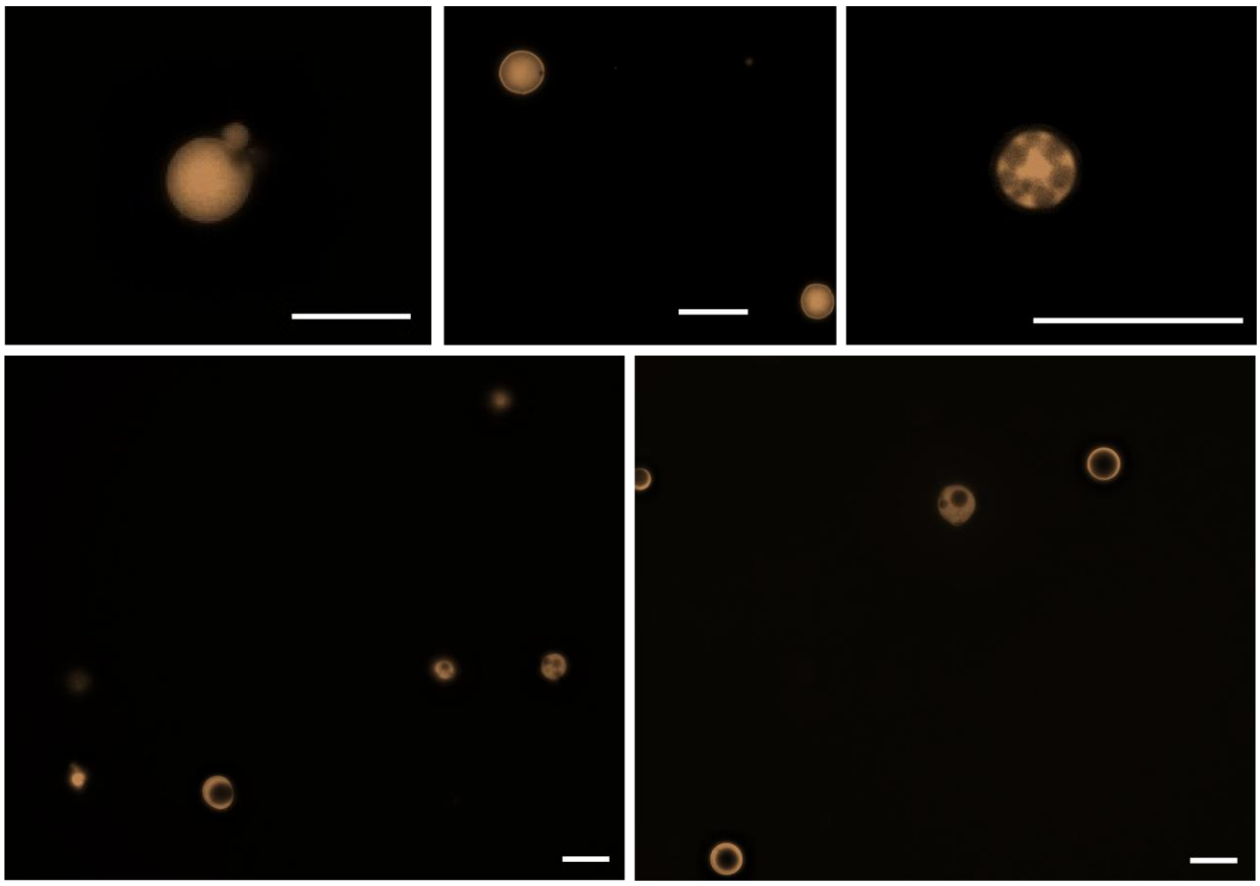

Figure S5 Fluorescence microscopy of a reaction starting with 0.5 M acetaldehyde and 5 % catalyst loading at room temperature which was sampled after 3 h. Orange color: rhodamine B fluorescence. Scale bar: 10 μm.

2.3.9 Various reaction conditions

To test robustness, the influence of salt additives, temperature and pH was investigated.

According to **GP1** the following reactions were conducted.

Table S14 List of tested reaction conditions using salts, temperature, and pH.

reaction condition	acetaldehyde concentration [M]	catalyst loading [%]	altered condition
27	1.0	10	400 mM NaCl
28	1.0	10	10 mM $MgCl_2$
29	0.5	5	40 °C
30	0.5	10	40 °C
31	0.5	5	0 °C
32	0.5	10	0 °C
33	0.5	5	pH 2.5 (AcOH)
10	0.5	5	pH 4.0 (AcOH)
34	0.5	5	pH 7.0

2.3.9.1. Salt content

Table S15 Light micrographs and HRMS measurements at 1.0 M acetaldehyde concentration and 10 % catalyst loading using 400 mM NaCl or 10 mM $MgCl_2$ after 1 h and 3 d respectively. Scale bar: 20 µm.

no.	micrograph		HRMS	
	1 h	3 d	1 h	3 d
27	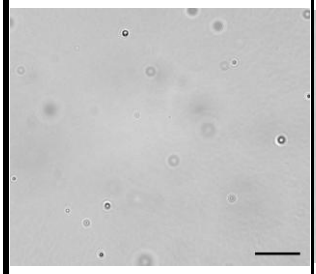	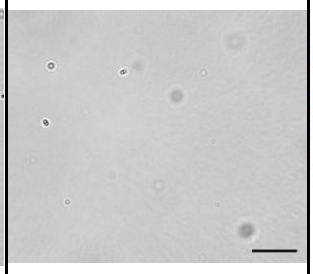	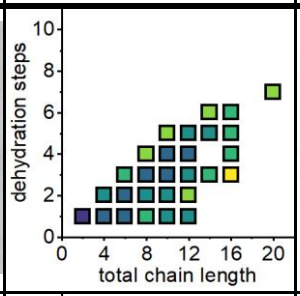	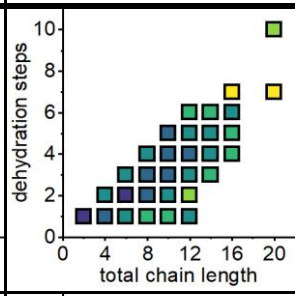
28	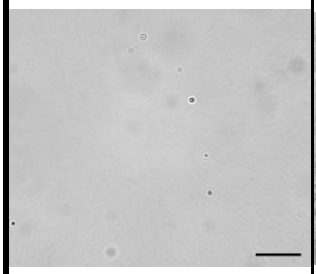	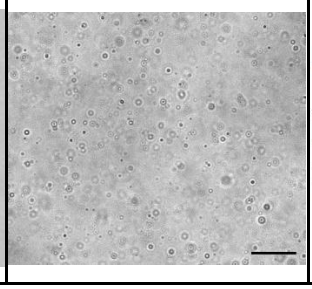	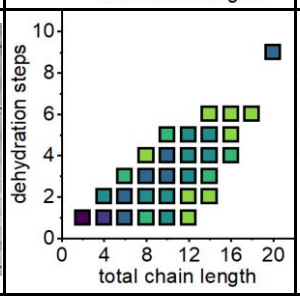	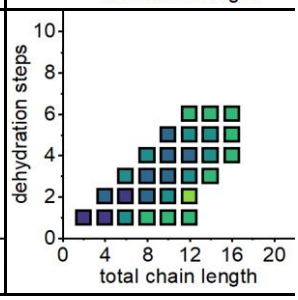
	for comparison reaction without salt additives after 1 h (see reaction condition 17, according to **GP1**)			
17	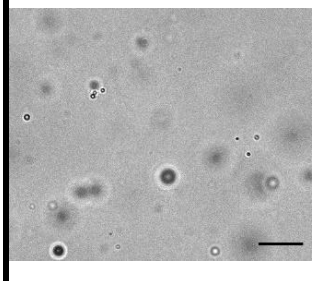		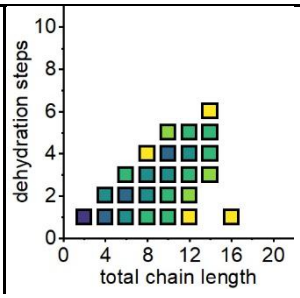	

To mimic the salt content in an early ocean, we used 400 mM for NaCl or 10 mM for $MgCl_2$. We observed that the addition of salts facilitated the oligomerization and elimination of water. This can be seen when comparing the 1 h measurements with the reaction condition **17**. The total chain length of 16 was already detected after 1 h, when a salt was present. However, the higher NaCl concentration led to the inhibition of macromolecular structures as the micrographs differ greatly between $MgCl_2$ and NaCl after 3 d. In contrast, $MgCl_2$ did not interfere with the formation, although as a bivalent cation it can disrupt membranes more easily.

2.3.9.2. Reactions at 40 °C

When keeping the reaction mixture at 40 °C, the size of some structures can be up to 5−10 µm and small spheres can be observed sticking to the surface or even being inside (**Table S16**). When using fluorescence microscopy (**Table S17**), spheres can also be observed inside the coacervates. Inside the dark spheres fluorescence is quenched by a polar environment. We conclude that the water, being produced during the condensation reactions, is accumulating inside the coacervates in the form of droplets. This is also highlighted in the Supplementary videos 3-5. An increase in volume of water droplets can also be observed over time. The coacervates with internal water accumulation are extraordinary since they help concentrating nonpolar, water-insoluble molecules inside along the polar water droplets which may accumulate themselves polar molecules from the environment, bringing these two compound classes together in a confined reaction space. In an extreme case (**Table S17**), reaction condition 30, 1 d) we were able to observe vesicle like structures, where the water content fully displaced the inside of the coacervate without collapsing the outer boundary/membrane. This transformation from a coacervate to a vesicle by internal water production has not been considered yet and may help close the gap between simple coacervates and more complex vesicles.

When comparing the HRMS data with the same reaction condition at room temperature (condition 10), it is clear that an increase in temperature also leads to an increase in reactivity. More and longer chain lengths are detected at elevated temperatures with shortened reaction times.

Table S16 Light micrographs of a reaction at 40 °C using a 0.5 M acetaldehyde concentration and 5 % or 10 % catalyst loading, respectively, after 1 h. Scale bar: 20 µm.

condition	micrographs 1 h		
29	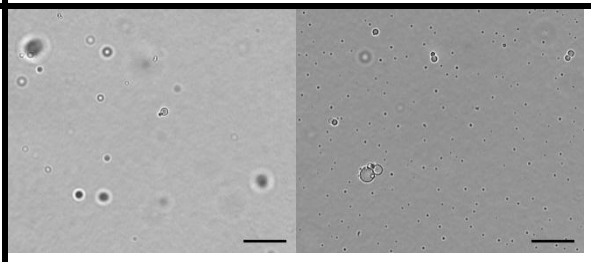		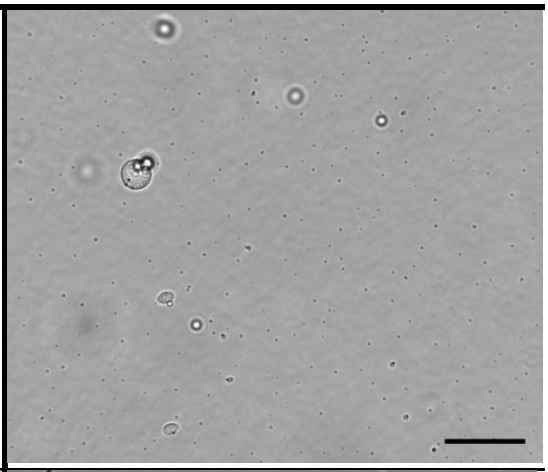
30	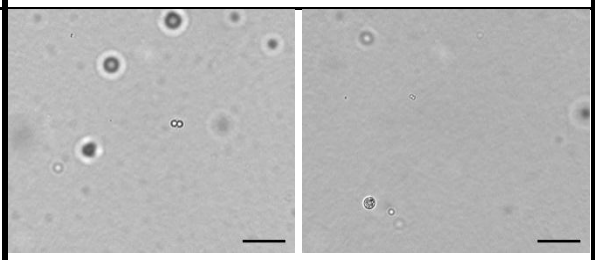		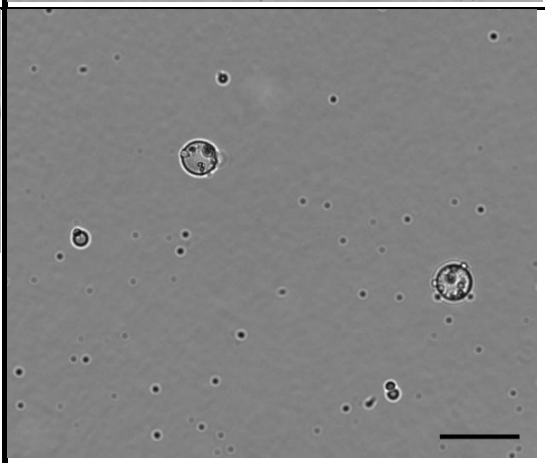

Table S17 Selection of fluorescence micrographs and HRMS measurements of a reaction at 40 °C using a 0.5 M acetaldehyde concentration and 5 % or 10 % catalyst loading, respectively. Rhodamine B: orange color. Scale bar: 20 µm.

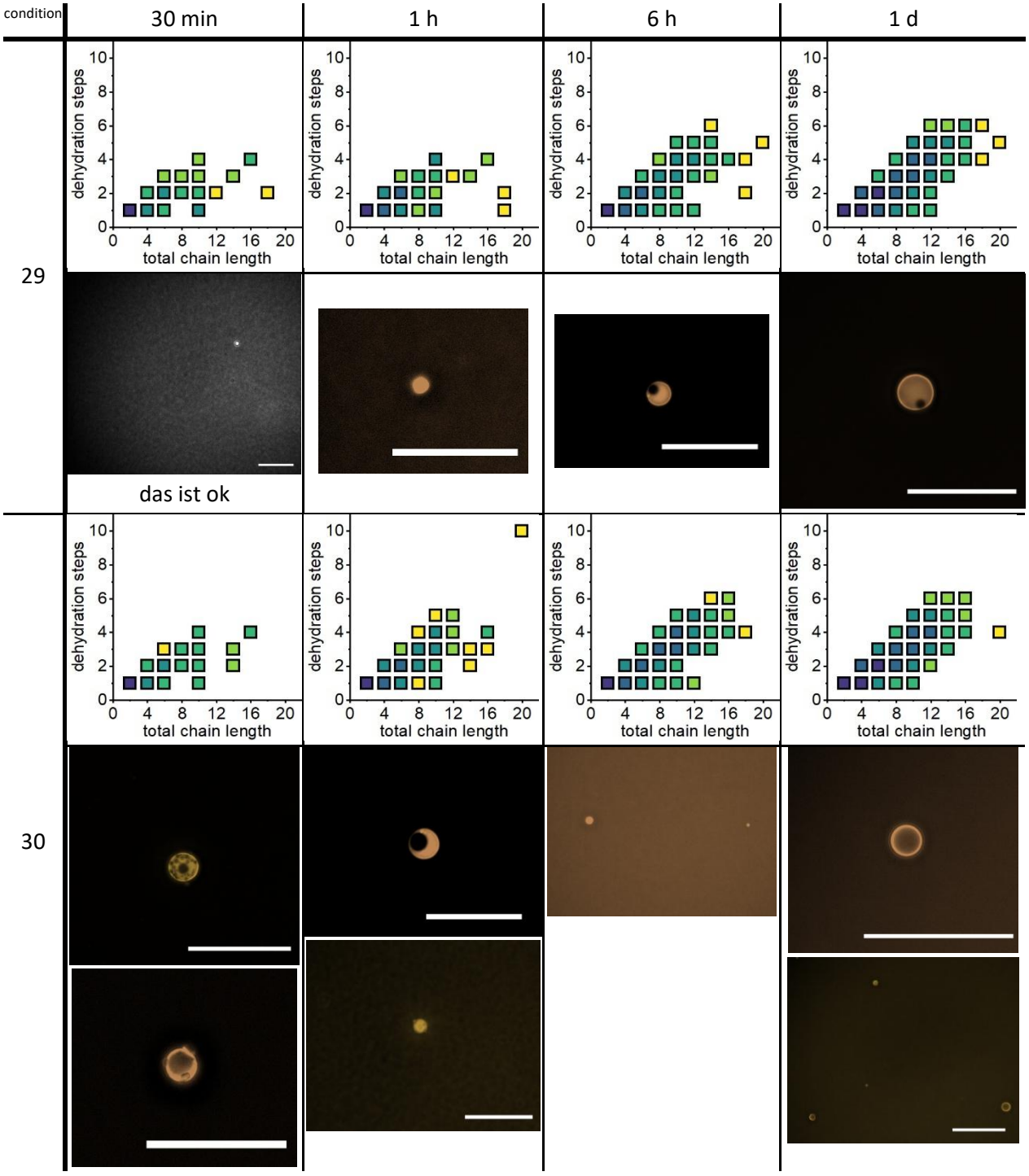

Table S18 Reference HRMS data from reaction condition 10 for comparison. A 30 min measurement was not conducted here.

condition	1 h	6 h	1 d
10	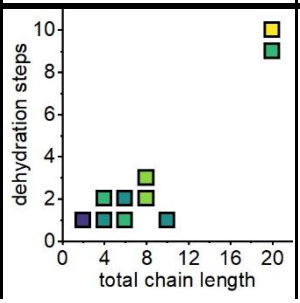	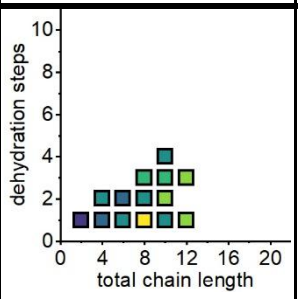	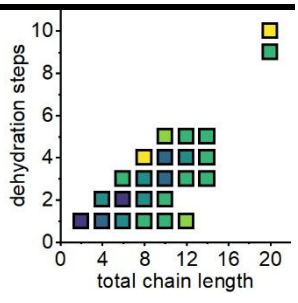

2.3.9.3. Reactions at 0 °C

Reactions at 0 °C (**Table S19**) resulted in a lower overall particle count after 1 h. Also, HRMS data showed reduced water elimination along an overall reduced oligomerization due to a lower reaction rate.

Table S19 Light micrographs and HRMS measurements at 0.5 M acetaldehyde concentration at 0 °C after 1 h and 5 % or 10 % catalyst loading, respectively. Scale bar 20 µm.

condition	micrographs	HRMS
	1 h	1 h
31	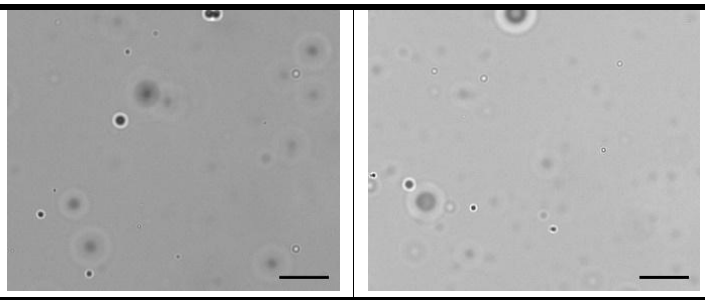	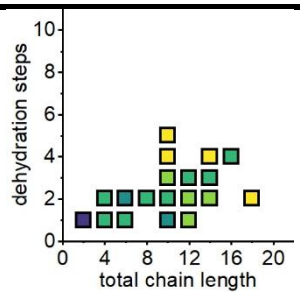
32	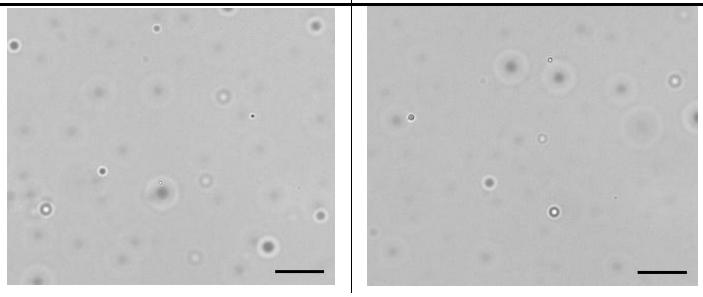	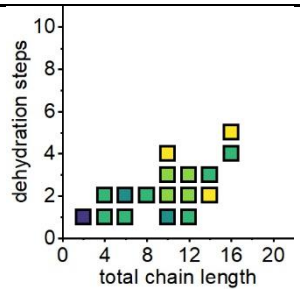

Table S20 Light micrographs and HRMS measurements at 0.5 M acetaldehyde concentration at 0 °C after 6 h and 1 d and 5 % or 10 % catalyst loading, respectively. Scale bar 20 µm.

cond.	micrographs		HRMS	
	6 h	1 d	6 h	1 d
33	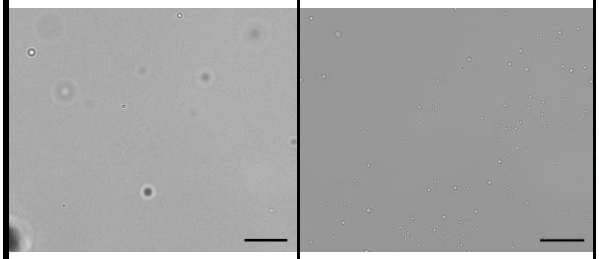		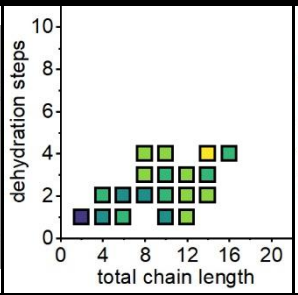	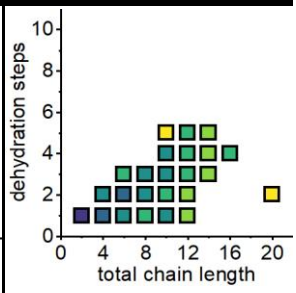
34	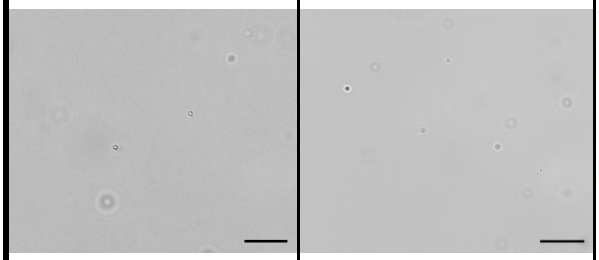		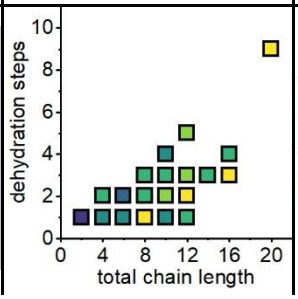	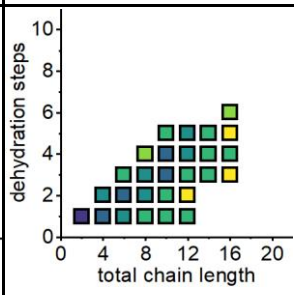

2.3.9.4. Reactions at pH 2.5, 4.0 and 7.0

When increasing or decreasing the pH, the particle count decreases significantly (**Table S21**). At lower pH (2.5, adjusted with AcOH) an increased oligomer length and water elimination was observed. In comparison, when we used pH 7, less water elimination and a lower oligomer length was observed. Here, the pH 4 was found to be optimal for particle formation and oligomerization.

Table S21 Microscope micrographs and HRMS measurements at 0.5 M acetaldehyde concentration and 5 % catalyst loading at pH 2.5, 4.0 and 7.0. Samples were taken after 1 h, 6 h, 1 d and 7 d, respectively. Scale bar 20 µm.

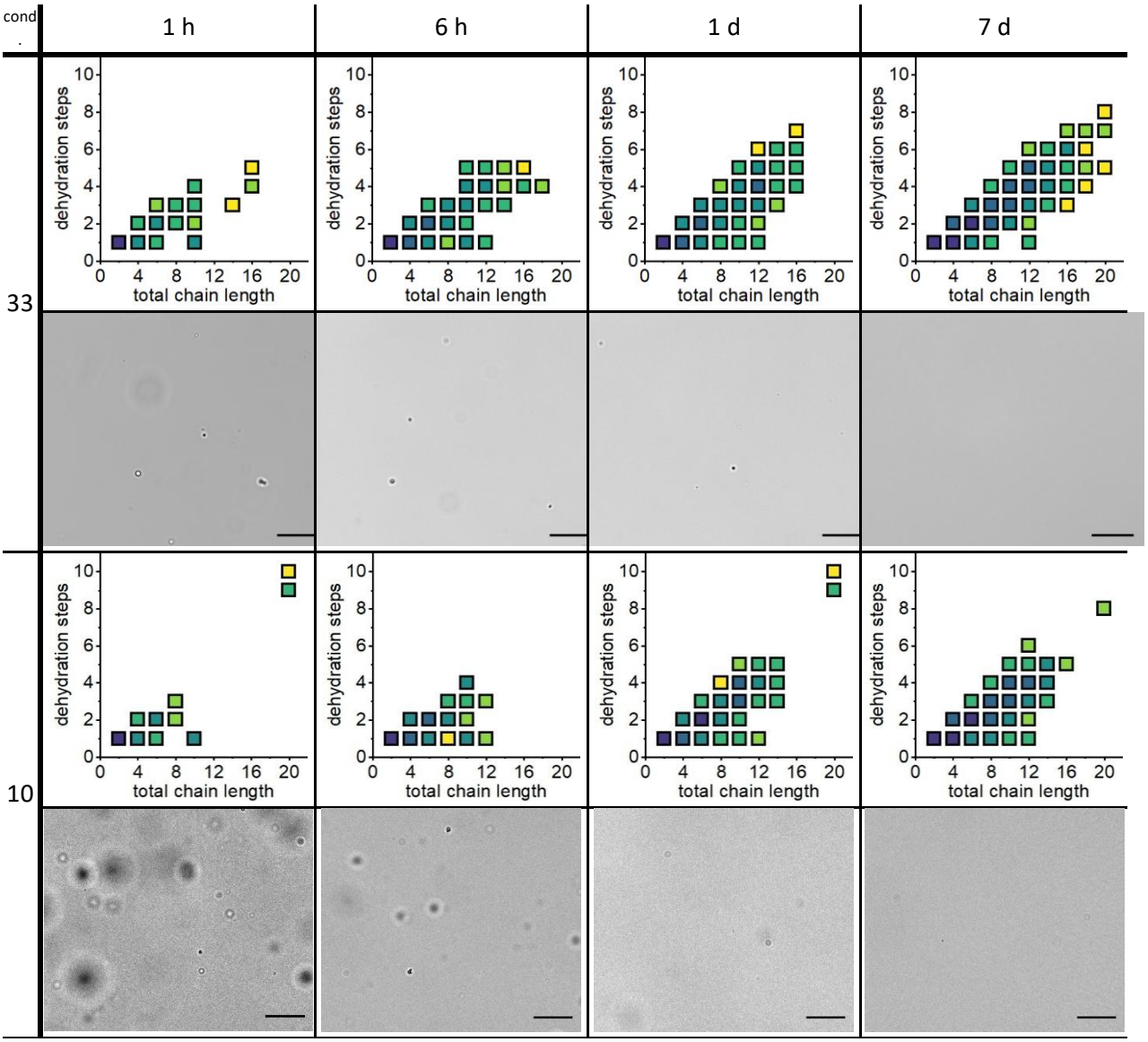

34

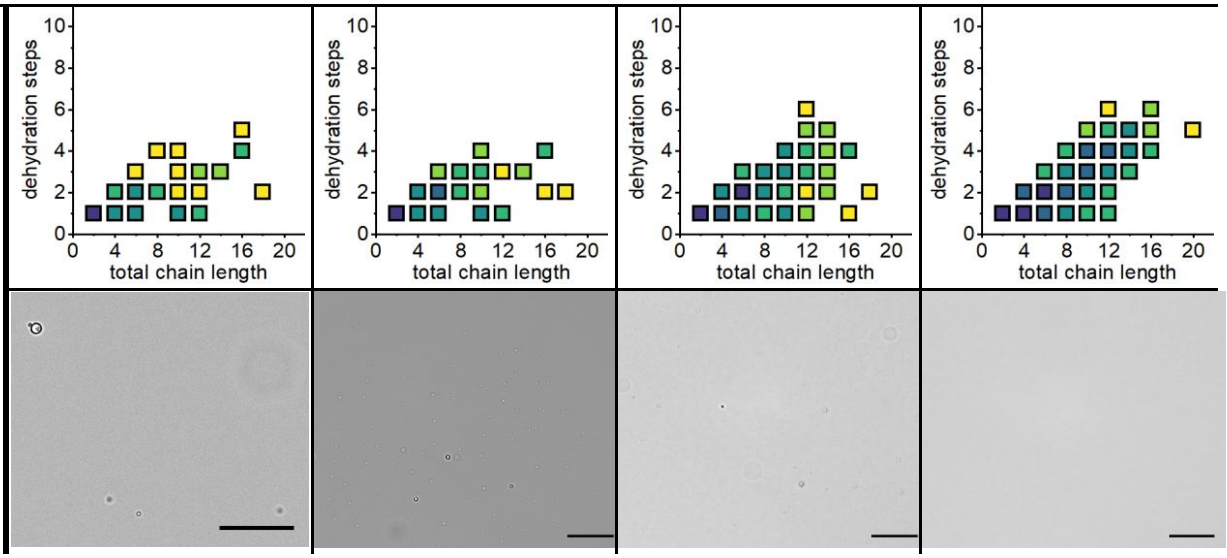

2.3.10 Dynamic light scattering (DLS)

The reaction was prepared according to **GP1**, then the reaction mixture was filtered by syringe filtration (0.45 µm cellulose acetate luer lock syringe filter, red, Ø = 13 mm). The solution was transferred to a cuvette and the measurement was started. For data acquisition, a *Viscotek 802 DLS* setup was used with the cell temperature set to 20 °C. The laser intensity was automatically adjusted to 300,000 counts prior to every data collection. Every 5 min a new data acquisition was started. The data was analyzed using the software "*OmniSIZE*" version 3.0.0.296 from *Viscotek*. Datapoints smaller than 1 µm were omitted due to solvent effects.

To track the whole process in a small timeframe, a high concentration of reagents was used. The linear plots of **Figure S6a** and **b** track the emergence and growth of two distinct particle sizes. The first species (**a**) starts growing from 100 nm whereas the bigger species (**b**) starts in the µm-range. It should be noted that the initial particle size can be smaller, as there is a time set-off between the start of the reaction and start of the measurement.

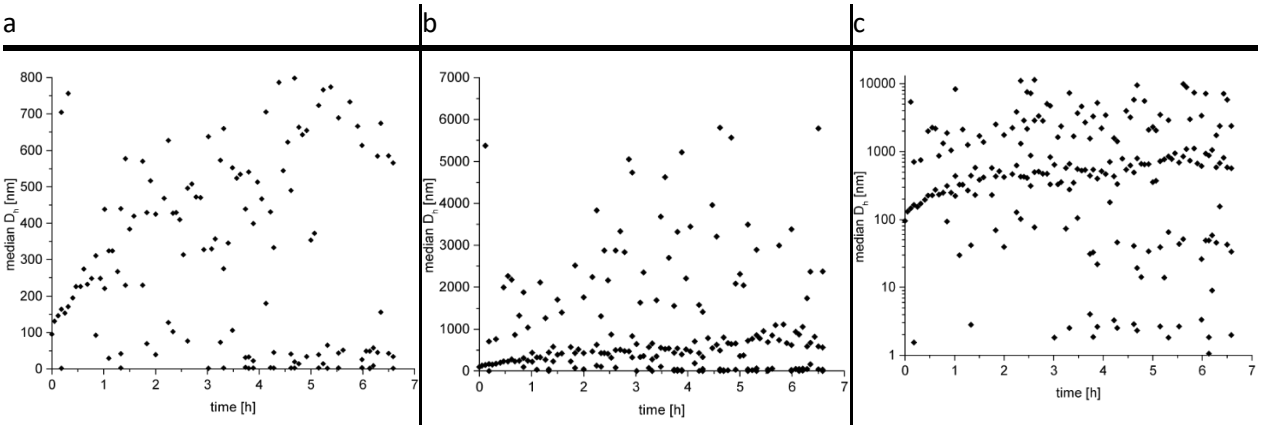

Figure S6 DLS plots of reaction condition 17 (1.0 M acetaldehyde concentration and 10 % catalyst loading) of the median hydrodynamic diameter D_h of particles found against time. a, linear plot up to 800 nm. b, linear plot up to 7 µm. c, logarithmic plot up to 10 µm. Data points smaller than 1 nm were omitted due to solvent effects.

3 TEM and cryo-TEM of the prebiotic reaction mixture

Table S22 Overview of conditions used for (cryo)-TEM setup.

reaction condition	acetaldehyde concentration [M]	catalyst loading [%]	experiment	sample taken
4	0.2	5.0	negatively stained using 2 % uranyl acetate on Quantifoil copper R3/3 holey carbon-supported grids	0 h, 1 h, 6 1 d
10	0.5	5.0	vitrified on Quantifoil copper R3/3 holey carbon-supported grids	1 h
10	0.5	5.0	vitrified on molybdenum grids coated with lacey films	1 h

When negatively staining a sample, large objects can locally displace uranyl acetate in the solution. When dried, the uranyl acetate left behind scatters the electron beam. In regions of displacement low scattering occurs which results in a lighter region, this results in a negative image of the sample. Therefore, only the outline of particles and not the internal structure can be examined by this method. In ***Figure S7*** spheres from ~100 nm of up to 1 µm in size can be observed. This also coincides with the DLS measurement which shows two growing species, one from ~100 nm and a bigger species in the µm-range. It should also be noted, that in all measurements uniform circles are present which are periodically manufactured holes in holey carbon-supported grids. The overview picture in the 6 h panel also shows these holes

0 h

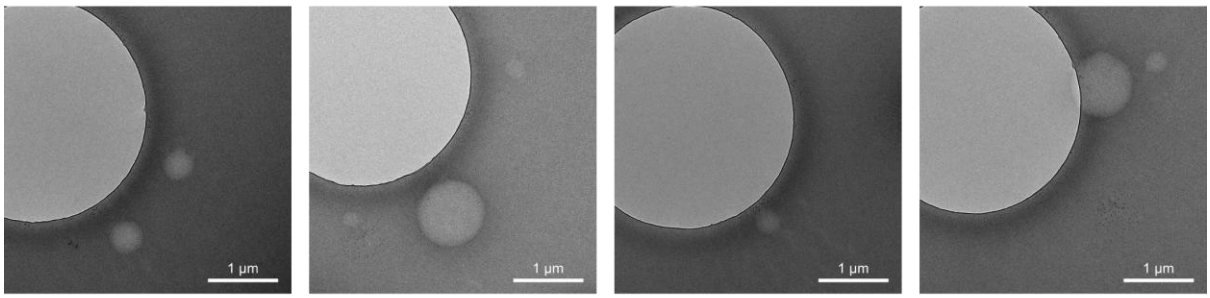
1 µm
1 µm
1 µm
1 µm

1 h

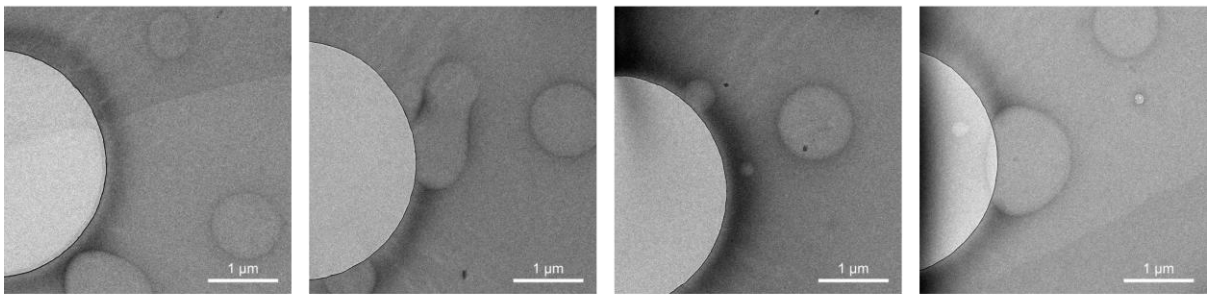
1 µm
1 µm
1 µm
1 µm

6 h

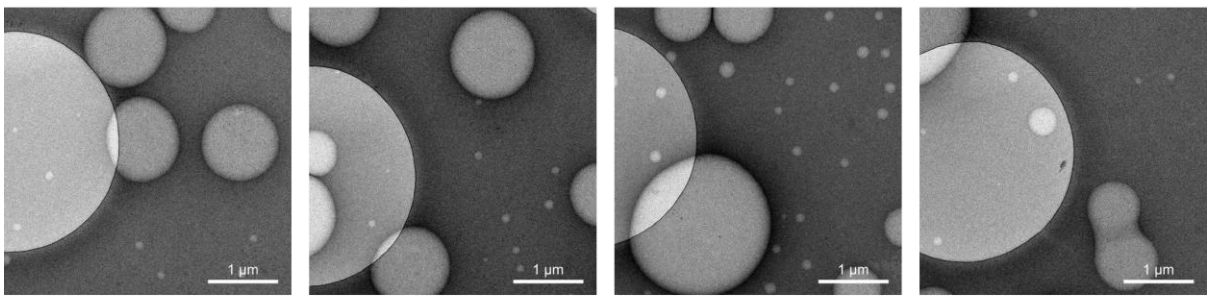
1 µm
1 µm
1 µm
1 µm

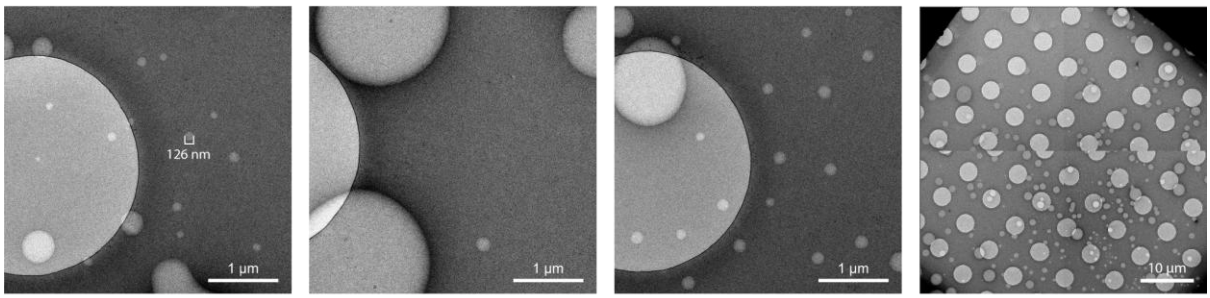
126 nm
1 µm
1 µm
1 µm
10 µm

1 d

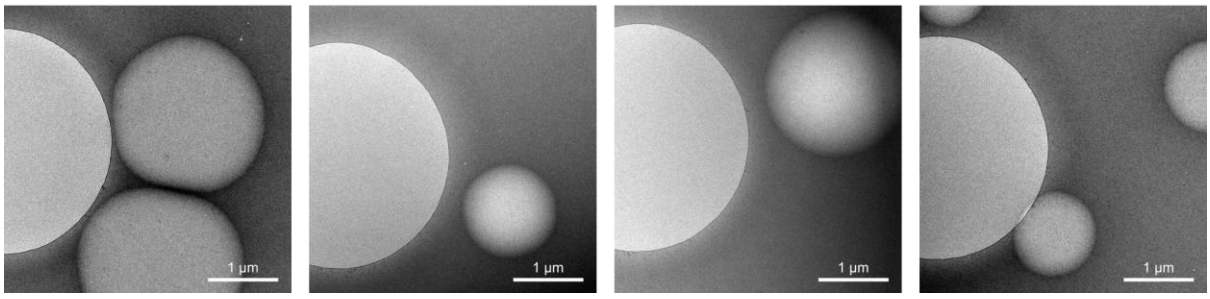
1 µm
1 µm
1 µm
1 µm

Figure S7 TEM images of negative stain after 0 h, 1 h, 6 h and 1 d. Negatively stained using 2 % uranyl acetate on Quantifoil copper R3/3 holey carbon-supported grids. Acetaldehyde concentration was 0.2 M and catalyst loading 5 %. Scale bar 1 µm except overview.

On Quantifoil copper R3/3 holey carbon-supported grids we were able to image vitrified samples with mostly coacervate like structures (**Figure S7**). These show a clear boundary but no (double)-membrane like structure is visible. However, in the first image in this panel we were able to observe a coacervate structure with darker spheres inside which can represent the local water accumulation during aldol condensation. The outer sphere also shows no sign of a double membrane, but a distinctive separation from the surroundings is visible.

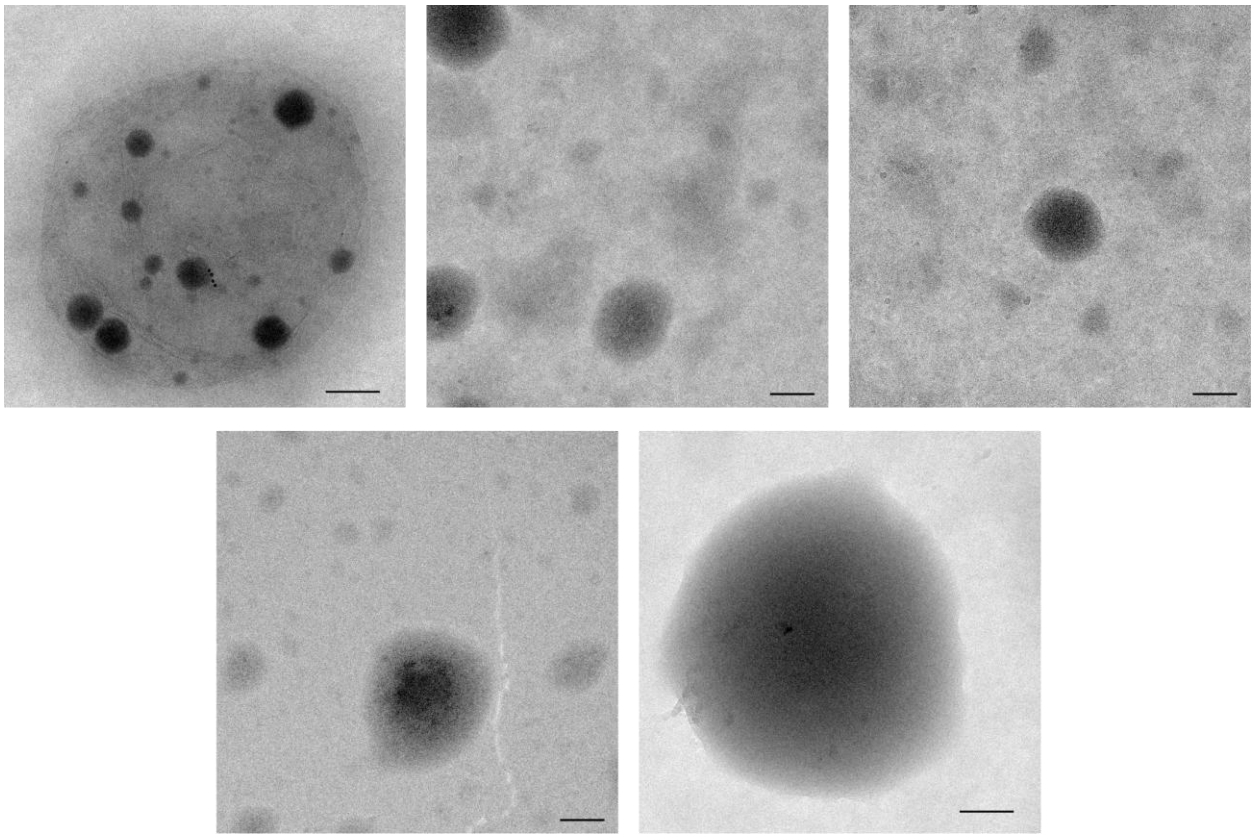

Figure S8 cryo-TEM images of a vitrified sample (on Quantifoil copper R3/3 holey carbon-supported grid) after 1 h reaction time. Acetaldehyde concentration was 0.5 M and catalyst loading 5 %. Scale bar 100 nm.

On molybdenum grids coated with lacey film (vitrified sample) we were able to observe another coacervate structure with dark spheres inside which indicate internal water production. In the right large sphere, we can observe a dark sphere which matches the internal curvature of the host sphere. Therefore, we can clearly confirm that the dark spheres are within the volume larger structure and not above or below. Additionally, significantly smaller spheres were also observed on the lacey grids. These structures are in the range of 11–40 nm and even smaller than the ones found in the negative stain or DLS experiment. We propose that these spheres are the first being formed during the reaction and then grow larger by accumulation of nonpolar material or combination with nearby spheres.

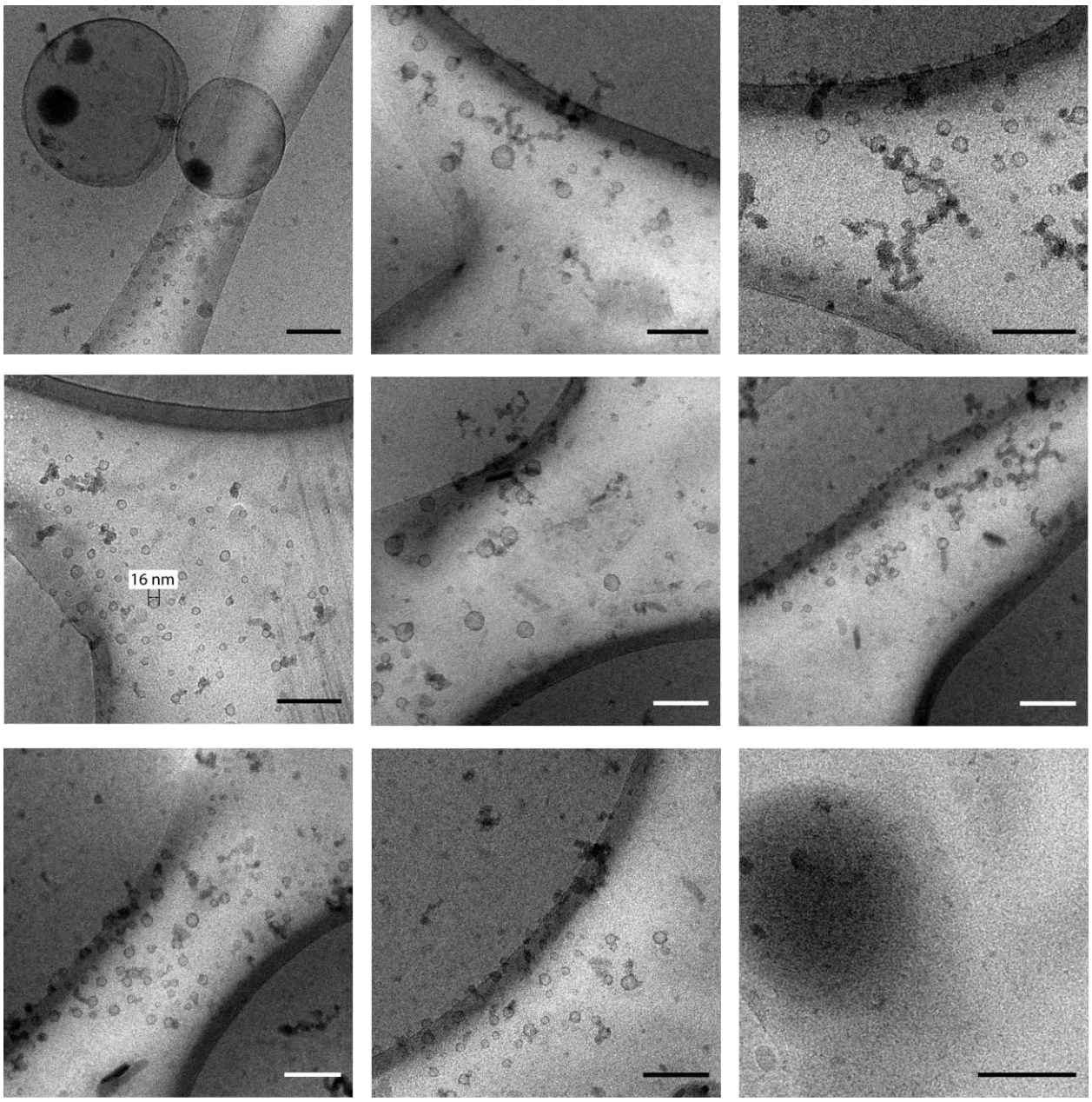

Figure S9 cryo-TEM images of vitrified sample (on molybdenum grid coated with lacey film) after 1 h reaction time. Acetaldehyde concentration was 0.5 M and catalyst loading 5 %. Scale bar 100 nm.

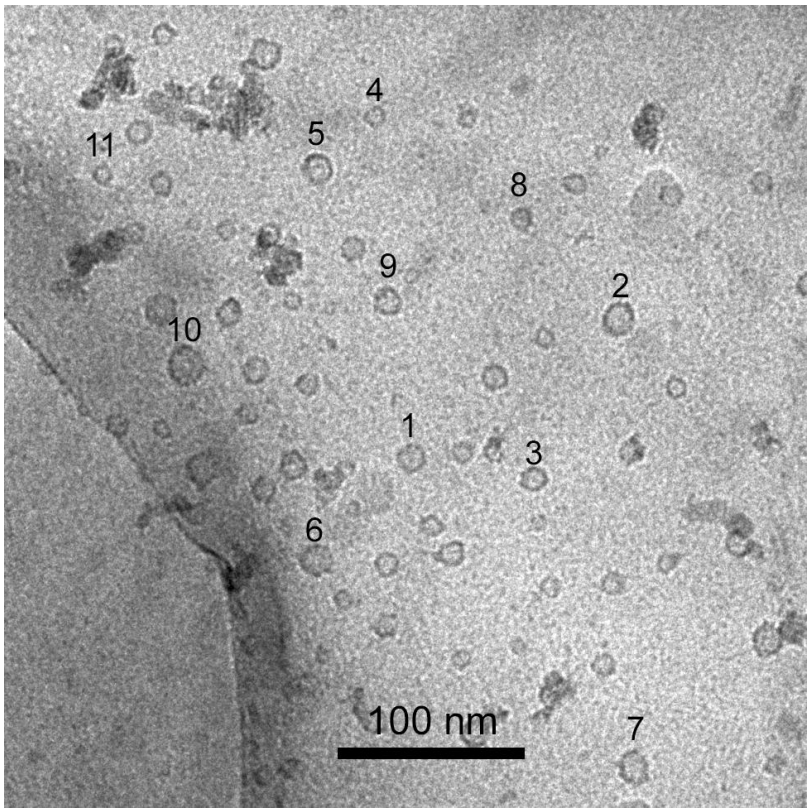

Figure S10 Part of center left panel of **Figure S9** with selection of 11 small assemblies for size and thickness measurements. Scale bar: 100 nm.

Table S23 Average diameter and average membrane thickness of a selection of small assemblies in **Figure S10**.

number	average diameter [nm]	average membrane thickness [nm]
1	15.99	2.86
2	18.61	3.52
3	14.25	3.14
4	11.77	2.75
5	17.20	3.12
6	17.59	3.29
7	18.31	3.12
8	12.35	2.71
9	15.75	2.95
10	21.18	3.02
11	11.00	3.21

The diameter of each sphere was measured three times and averaged. The membrane thickness of each sphere was also measured in three points and averaged. It should be noted that the membrane thickness did not change with increasing sphere diameter. In addition, the average over all membrane thicknesses was calculated. We obtained the overall membrane thickness as 3.06 nm ± 0.24 nm.

4 NMR spectra of synthesized compounds

4.1 *tert*-butyl (*S*)-(1-amino-1-thioxopropan-2-yl)carbamate (9)

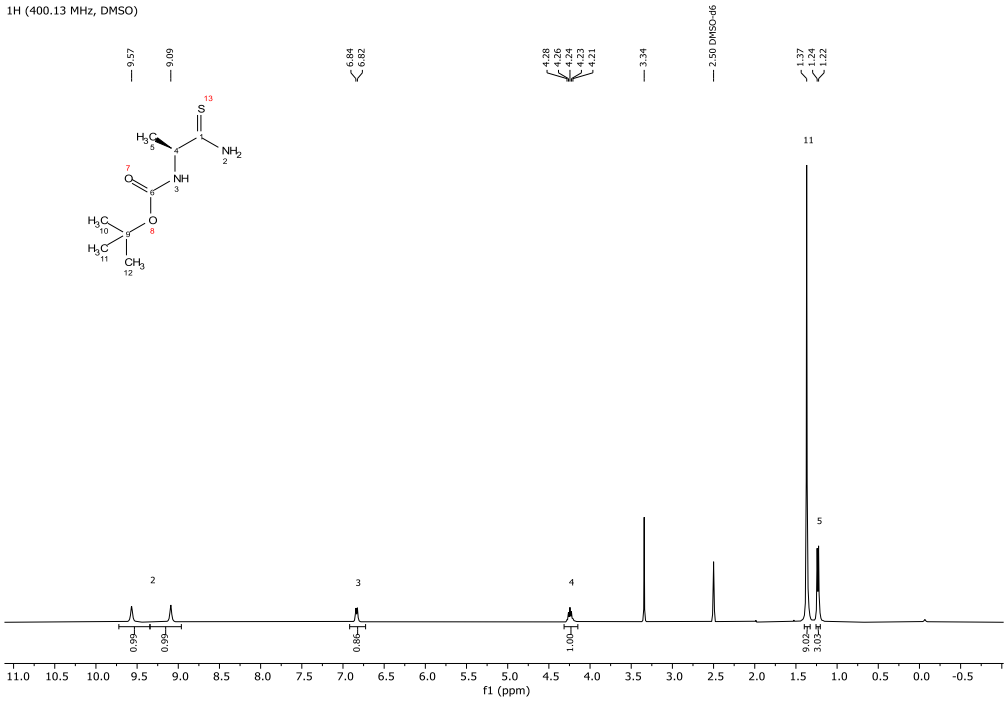

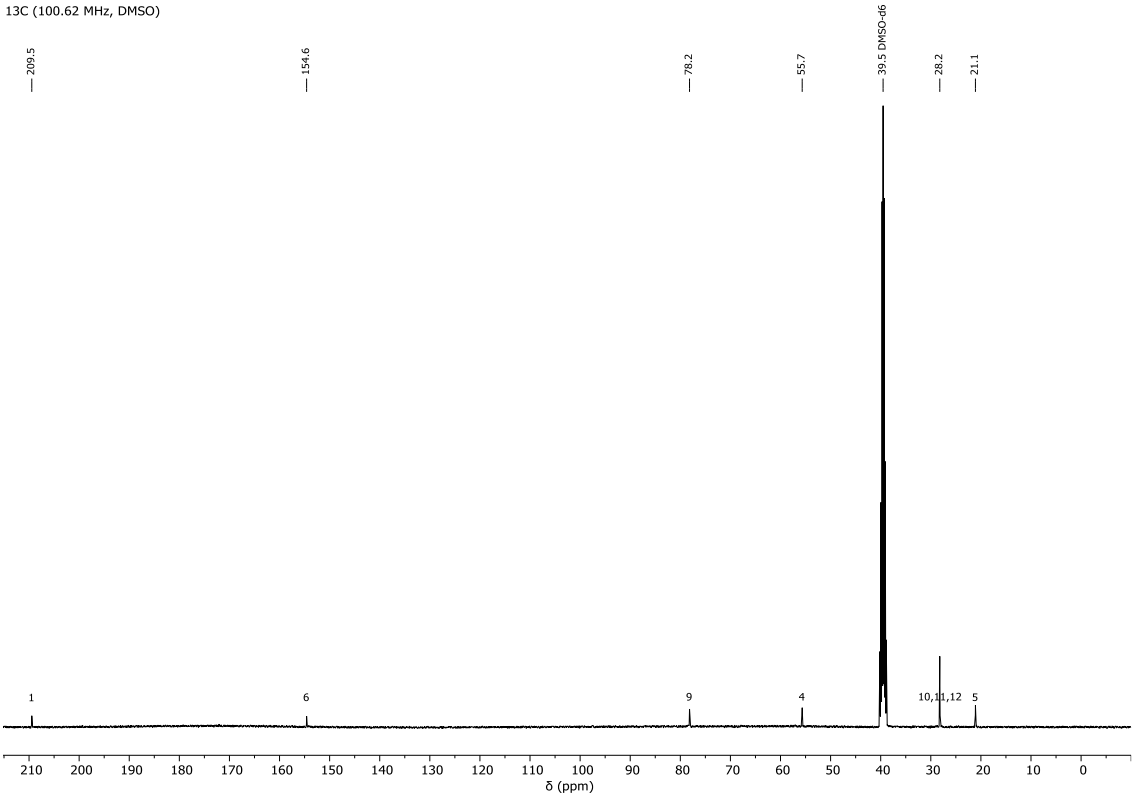

4.2 (*S*)-2-aminopropanethioamide hydrochloride (8-HCl)

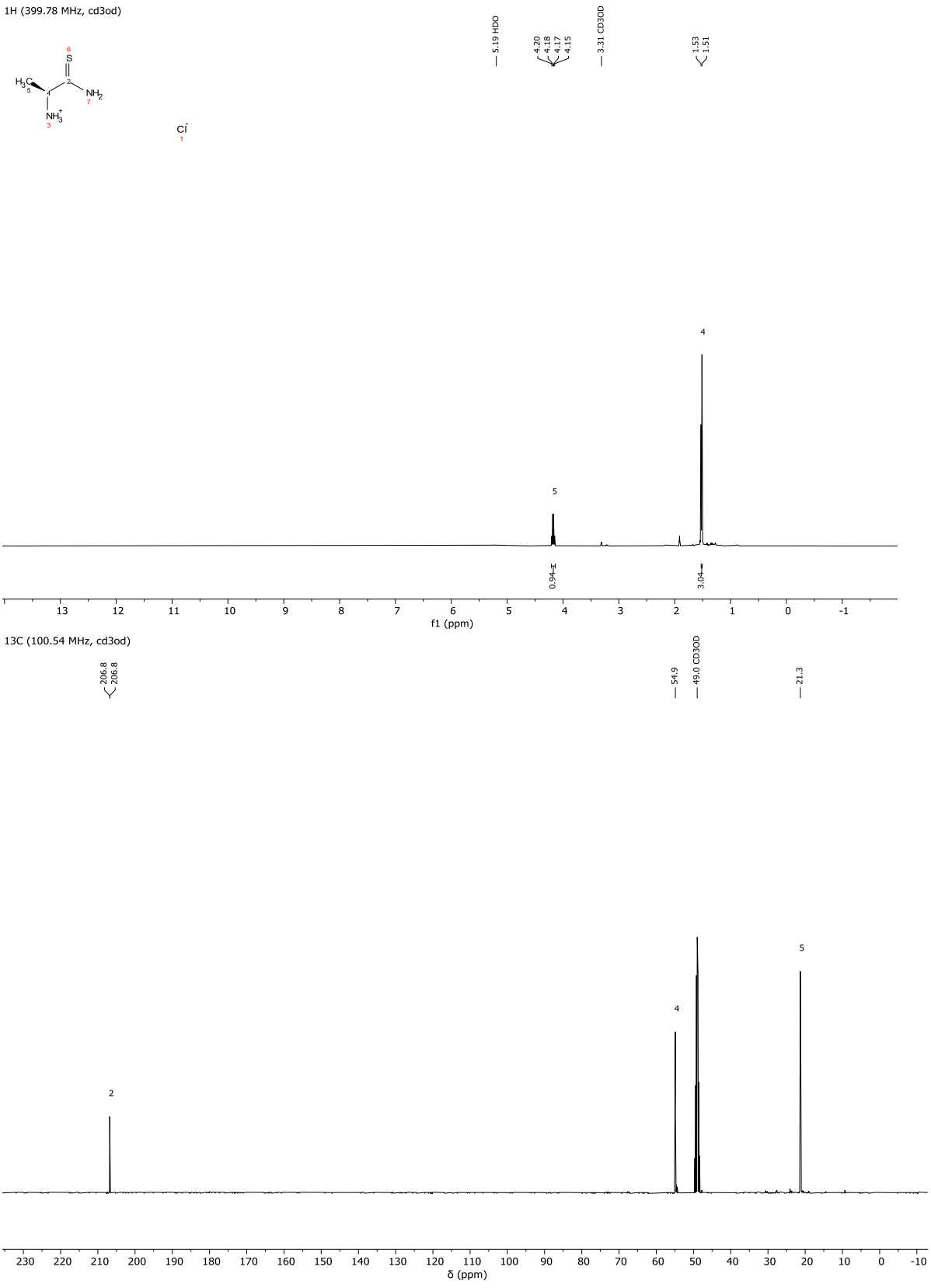

4.3 (5*S*)-2,5-dimethylimidazolidine-4-thione (1)

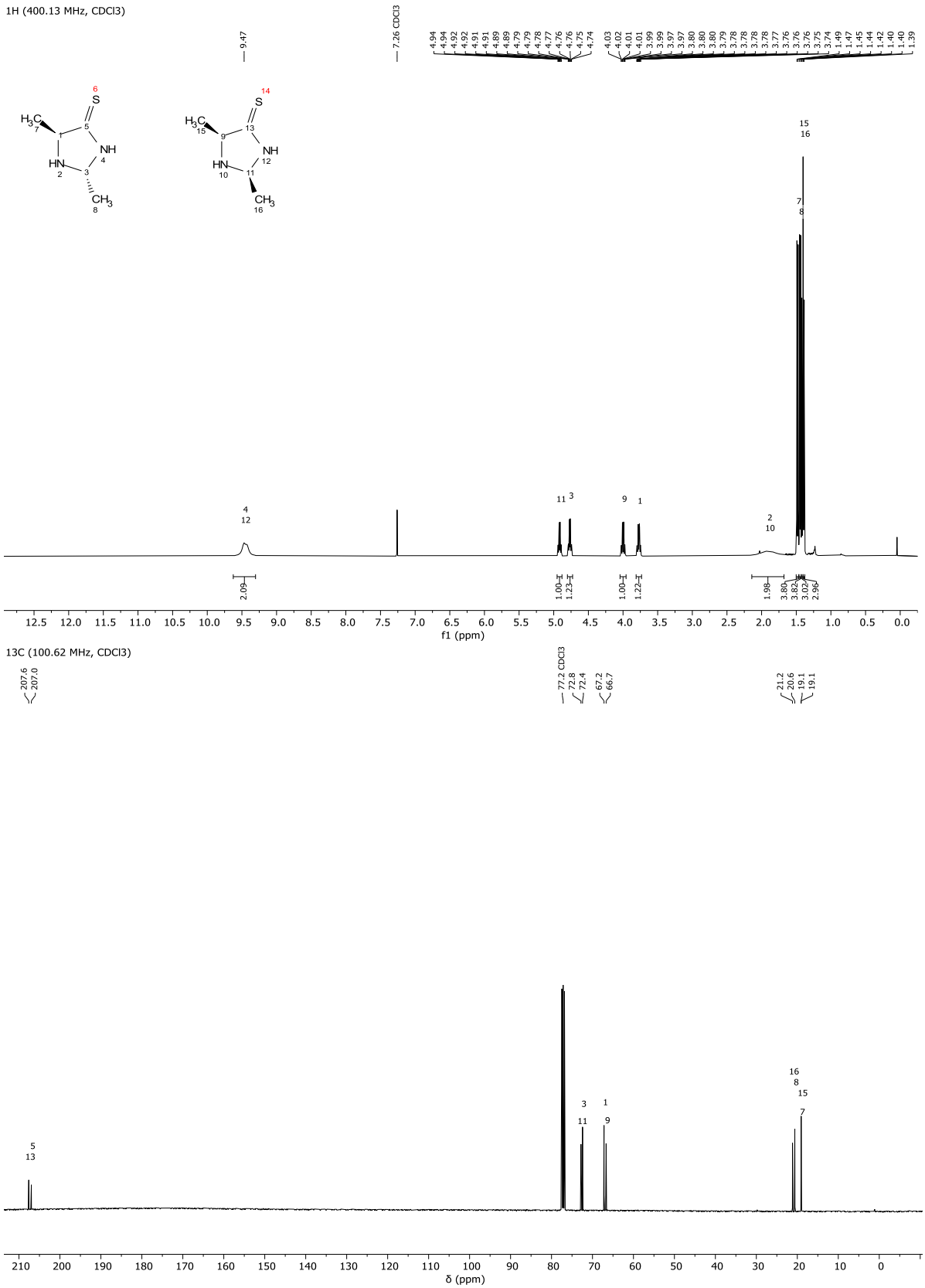

[1] G. R. Fulmer, A. J. M. Miller, N. H. Sherden, H. E. Gottlieb, A. Nudelman, B. M. Stoltz, *et al.* NMR Chemical Shifts of Trace Impurities: Common Laboratory Solvents, Organics, and Gases in Deuterated Solvents Relevant to the Organometallic Chemist. *Organometallics* **29**, 2176–2179 (2010). https://doi.org/0.1021/om100106e

[2] Chambers, M., Maclean, B., Burke, R. *et al.* A cross-platform toolkit for mass spectrometry and proteomics. *Nat Biotechnol* **30**, 918–920 (2012). https://doi.org/10.1038/nbt.2377.